CELL KINETICS AND TRACK STRUCTURE

John W. Wilson, F. A. Cucinotta, and J. L. Shinn

NASA Langley Research Center
Hampton, VA, U.S.A.

ABSTRACT

A major uncertainty in shield requirements for deep-space missions is establishing biological risk for high charge and energy (HZE) exposure. Estimates of biological risk in space requires an understanding of the relationship of ground-based biological experiments with intense particle beams to the low exposure rates in the space environment. We have examined the relation of a (relatively) general cell kinetic model to the track structure theory of Katz and determined repair coefficients from the experiments of Yang et al. as a means of predicting biological response to low dose-rate exposure in the deep-space environment. The model provides repair dependent relative biological effectiveness (RBE's) which agree well with values found in ion exposure experiments and makes predictions which could be tested in future laboratory studies. The model seems to provide the necessary requirement of relating laboratory response data to space exposure conditions with the exception of the gravity environment effects.

INTRODUCTION

Before sending men into deep space for more than several months, there are many issues concerning radiation safety of the high energy and charge ions (HZE) of the galactic background radiation (Grahn, 1973) which must be resolved. The preponderance of human data available on radiation exposure is from (mainly) γ-ray exposure data obtained from the nuclear weapons of World War II (BEIR V). These are augmented by biological experiments for various radiation types in search of a means of extrapolating the human risk data for γ-rays to any arbitrary radiation field (Sinclair, 1985). This is the origin of the quality factor (Q) based on experimentally observed relative biological effectiveness (RBE) for various radiation exposure types. Central to the development of this method of estimating radiation protection requirements is the assumption that the experimental RBE reaches a maximum value as the delivered dose approaches zero independent of the dose rate at which the experiment was performed (ICRU, 1986). Such an assumption depends on the biological repair rates and repair efficiencies and there is evidence that the maximum RBE may not be practically achievable in laboratory experiments for some biological systems (Wilson and Cucinotta, 1991). Furthermore, very large RBE values have already been observed for some biological systems (Merriam et al., 1984; Thomson, Williamson and Grahn, 1989) that if implemented into this conservative protection methodology based on Q then the implementation of deep space travel would be difficult to achieve. Clearly, the resolution of these issues is of the utmost importance to the future of NASA's manned space program.

Biological Effects and Physics of Solar and Galactic Cosmic Radiation, Part A, Edited by C.E. Swenberg *et al.*, Plenum Press, New York, 1993

The present work is an outgrowth from a request by the Life Sciences Branch to develop methods of extrapolation of laboratory experiments to long duration space exposure. Most of that work was accomplished with disregard to the role of biological repair mechanisms (Wilson et al., 1990; Cucinotta et al., 1991) which would have a limited role in most laboratory experiments but is of critical importance in the low level space environment (17 μGy/hr). To address this issue we implemented a cell kinetic model based on a simple analogy with chemical kinetics (Frost and Pearson, 1962) motivated by the belief that the ultimate cell repair mechanisms are chemical in nature (Wilson and Cucinotta, 1991). At the same time, our awareness of the complexity of rather simple chemical systems (Wilson et al., 1984) especially those excited by ionizing radiation (Wilson, DeYoung, and Harris, 1979) gives us pause in approaching such a complicated chemical system as a living cell where thousands of chemical species are inhomogenously mixed even prior to radiation exposure. Clearly, there must be a great simplification in approaching this problem if any analytic expression is to be derived concerning radiation response.

There are essentially three types of kinetic models which have been used in past studies (Tobias, 1985; Goodhead, 1985; Scott and Ainsworth, 1980). The first two models evaluate the average number of lesions per cell and assume nonlinear kinetic terms as the source of sigmoid behavior in the survival curve. The repair-misrepair (RMR) model (Tobias, 1985) assumes a linear repair kinetic term to remove lesions (sublesions) from the cell, while a binary misrepair kinetic term produces lethal lesions appearing as lack of biological survival. A later version of the model assumes that sublesions can be "fixed," presumably as the cell progresses (Curtis, 1986). The binary misrepair term has been shown to be relatable to the dual action response model (Curtis, 1986) and the multitarget theory of Katz et al. (1981). A second nonlinear kinetic model assumes that repair enzymes are depleted in the repair process so that at large exposure levels the repair rates decrease to zero (saturated repair) as the repair enzyme pool is depleted (Goodhead, 1985). The unrepaired damage is assumed to be "fixed" at cell cycle progression when inactivation is expressed. Although the mechanisms are substantially different, both models describe well the sigmoid behavior and dose-rate-dependent response of mammalian cell cultures. Linear kinetic models (called state vector models) have found application in the literature (Scott and Ainsworth, 1980) and are adaptable to inclusion of cell environmental effects (Crawford-Brown and Hoffmann, 1990). The state vector models are closely related to the multihit model (Casarett, 1968). The main success of the two nonlinear models and the state vector model is for x-ray exposures. There is no clear development of these models to include track structure effects in heavy ion exposures.

It is well known that nonlinear processes dominate at high power densities in chemical processing (for example, Wilson, 1980; Wilson and Lee, 1980). Two and three body recombination processes are well known examples of nonlinear processes (Wilson, DeYoung and Harris, 1979). Chemical combinations of reactive species are present even at the lowest power levels where they tend to dominate and often follow linear kinetic equations (Wilson and Lee, 1980). High density power levels are locally present with the passage of high LET particles even at low exposure rates so that chemical products at high power with low LET radiation are similar to those produced by even low exposure levels of high LET radiation (Charlesby, 1967). Such facts have long been known to radiation chemist for high LET neutron environments at nuclear reactors. Similar nonlinear processes are related to the columnar recombination in ion chamber and scintillator detectors resulting in reduced detector efficiency. Any viable radiation model must account for the high power densities within particle tracks but the nonlinear time scale within the track chemistry is (very) short compared to the time scale of subsequent biological repair mechanisms giving hope that the repair kinetics may yet be describable by a linear kinetic model (Ngo et al., 1990) in which nonlinear processes are ascribed to mainly track structure effects. The veracity of such an approach would lie with the observed biological response under varied exposure conditions and the role of modeling would be to help define critical experiments. It is our hope that the low dose and low dose rate inherent in most space exposure can be adequately described by linear repair kinetics with nonlinear behavior confined to track structure effects as motivated by the above considerations.

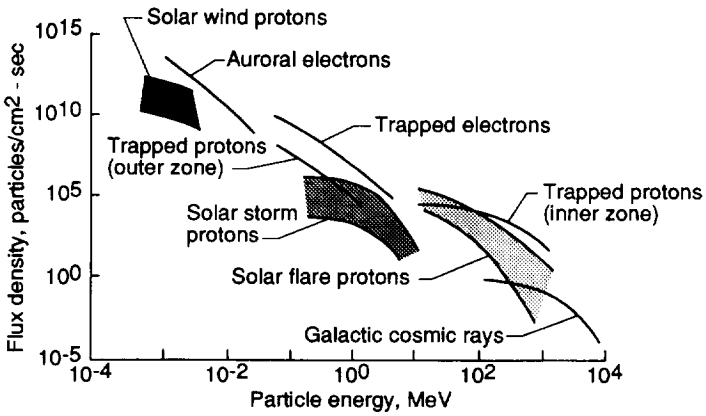

Figure 1. Space-radiation environment.

There is ample evidence that radiation injury to cell membranes and cytoplasmic material is only effective at doses in excess of tens of Gy (Casarett, 1968). Such high exposures are associated with early lethality and of little relevance to normal space exposure. The normal doses in space are much less than 10 Gy and relevant biological effects are expected to occur many years after exposure. There will be no directly observable changes in tissue systems during or immediately after the flight. Rather subtle changes in cell chemistry have occurred which will not be fully expressed until much later in the life of the cell line or the individual. It is believed that such changes are related to changes in the DNA structure. This will be the assumption of the present work.

A multitarget model with track structure derived by Katz et al. (1971) has been quite successful in describing track-structure-dependent phenomena in biological cell systems (Waligorski et al., 1987). The model considers the simple physical arrangements of sensitive sites required for some observable to be manifest and a physical model for the energy deposited around the path of a moving charged particle. The effects of charged-particle irradiation are correlated with that of gamma-ray irradiation by assuming that the response in sensitive sites near the particle's path is part of a larger system irradiated with gamma rays at the same dose (Katz et al., 1971). In the Katz model, mechanistic assumptions are avoided. The parameterization of the response to gamma rays provides for calibration of a biological systems response, as well as a transfer function for describing heavy ion effects. The main criticism of the model is its inability to predict repair-dependent phenomena (Curtis, 1986; Lett et al., 1989) and failure to achieve a maximum RBE at low exposure.

In a previous report (Wilson and Cucinotta, 1991), we presented a simple phase dependent repair model in which track structure effects were added through the use of the Katz formalism. Repair coefficients were estimated from the experiments of Yang et al. (1989) on stationary G_1 mouse cells in which varying amounts of repair in G_1-phase was allowed before cell cycling. Highly efficient repair was demonstrated for G_1-phase for light ions while high energy ^{56}Fe exposures showed little repair in good agreement with the kinetic model.

INTERACTIONS AND KINETIC PROCESSES

The energetic particles in space consists of mainly atomic constituents covering a very broad energy spectrum and flux values as shown in figure 1 (Wilson, 1978). The particles themselves are small ($\approx 10^{-13}$ cm) but are electrically charged resulting in a long-range force component. A casual look at condensed matter reveals mostly the structure of the electron clouds which contain only 0.05 percent of the mass but occupy virtually all the space within the material. Embedded within these electron clouds are the atomic nuclei whose dimensions

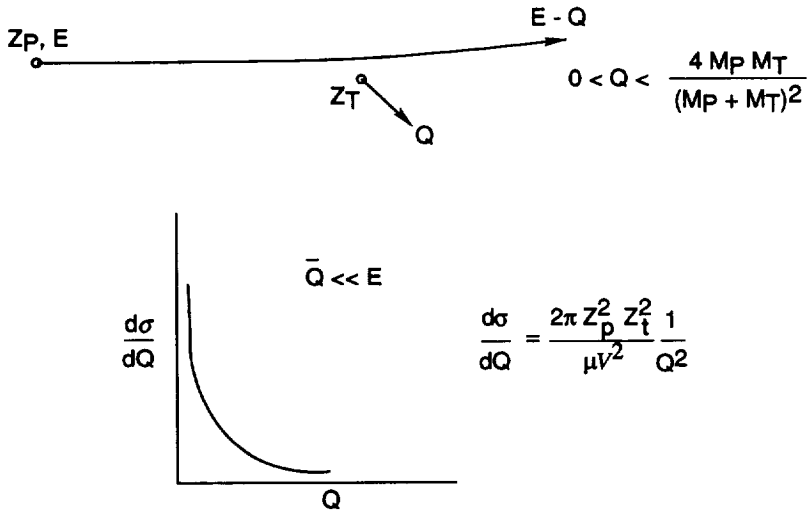

Figure 2. Coulomb scattering.

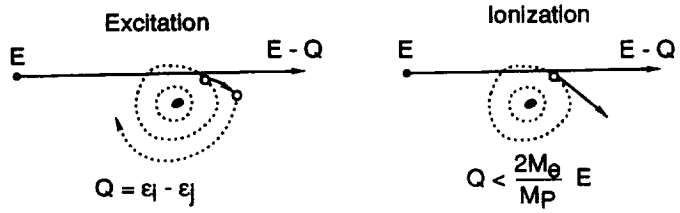

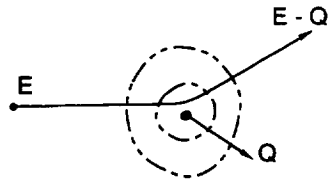

Figure 3. Schematic of Coulomb interactions with atomic electrons and atomic nucleus.

are 10^{-5} times smaller than the complete atom but contain 99.95 percent of the mass of the atom. Clearly an energetic particle passing through such a material will mainly interact with the electrons in the cloud and seldom strike a nucleus.

The dominate energy transfer process is energy loss through ionization, that is, a collision between the incoming charged particle (whether it is a proton, electron, or heavy ion) and the orbital electrons of the shielding material (fig. 2). They interact through Coulomb scattering, and the energy transferred from an ion of energy E and charge Z_p to a target particle of charge Z_t is labeled Q. The cross section σ has an inverse Q^2 dependence, and therefore the energy transfer is usually quite small. In the figure, μ is reduced mass for the projectile target system of masses M_P and M_T.

When the target is an electron bound in an atomic orbital, there are two options of either producing excitation when specific energy transfers ($\epsilon_i - \epsilon_j$, where ϵ_i and ϵ_j denote atomic energy levels) are made or ionization where the energy transferred must be greater than the ionization potential (fig. 3). The cross section is related to this energy transfer and goes like the inverse of Q^2. Another important process, especially for incident electrons, is Coulomb interaction with the atomic nucleus which results in multiple scattering effects. These multiple scattering effects are important for electron diffusion within the media.

The cross sections for secondary electrons produced from impacts of ions with atoms as described in figures 2 and 3 are shown in figure 4. This figure shows curve fits to the experimental data for 1 and 5 MeV proton impact (Manson et al., 1975), and the inverse Q^2 dependence above about 20 eV for the secondary electron energy is clearly evident. The corrections below 20 eV are due to binding effects which can only be treated quantum mechanically. The electron is actually bound in an atom, and these binding effects become important when the energy transfer is on the order of the binding energy. This type of data is important in giving the lateral spread of the energy from the track as the particle passes through a material.

There are added degrees of freedom when atoms are bound into molecular systems. Shown in figure 5 is a collection of data for N_2 molecules, which we chose as a typical molecule mainly because we could find the most data for it. This molecule has been under extensive investigation because of its importance to high power lasers and atmospheric phenomena. Vibrational excitation is important for electron energies below about 10 eV. Once the electronic excitation or ionization threshold is exceeded, the cross sections become heavily dominated by those two processes alone. In about one half the cases, ionization results in dissociation; and according to the data we have been able to collect, most molecules undergoing electronic excitation result in dissociation. There are, however, considerable differences in the dissociation cross section for these two processes as shown in figure 5. These differences are probably due to the small number of molecular states observed in the experiments. The molecular excitation cross section will probably change as further experiments are performed and the total electronic excitation cross section will probably show the same energy dependence as the ionization cross section at high energy. The data are taken from Schulz (1976), Cartwright et al. (1977), Köllman (1975), and Wight, Van der Wiel, and Brion (1976). The problem of molecular binding effects is difficult to treat using quantum theory but local plasma models have shown some success in treating both the molecular binding problem (Wilson and Kamaratos, 1981; Kamaratos, 1982; Xu, Khandelwal, and Wilson, 1984a and 1984b; Xu et al., 1984) as well as condensed phase effects (Wilson et al., 1984; Xu, Khandelwal, and Wilson, 1985).

Although most collisions in the material are with orbital electrons, the rare nuclear collisions are of importance because of the large energy transferred in the collision and the generation of new energetic particles. This process of transferring kinetic energy into new secondary radiations occurs through several different processes, such as direct knockout of nuclear constituents, resonant excitation followed by particle emission, pair production, and possible coherent effects within the nucleus. Through these processes, a single particle incident on the material may attenuate through energy transfer to electrons of the media or generate a multitude of secondaries causing an increase in exposure (transition effect). Which process dominates depends on energy, particle type, and material composition. This development of cascading particles is depicted in figure 6 as a relative comparison between high-energy proton and α-particle cascades in the Earth's atmosphere. Note the similarities displayed in figure 6 for individual reaction events and the nuclear-star events as seen in nuclear emulsion.

Neutrons and γ-rays are produced in local shield material and by local manmade sources such as nuclear power reactors. The neutrons interact through nuclear reactions similar to energetic protons whereby secondary charged particles are produced. The γ-rays interact through three main processes. The photoelectric cross section above ionization threshold, Compton scattering above tens of thousand electron volts and pair production above 1 MeV. The neutron induced nuclear stars are highly ionizing local events. The γ-ray produced

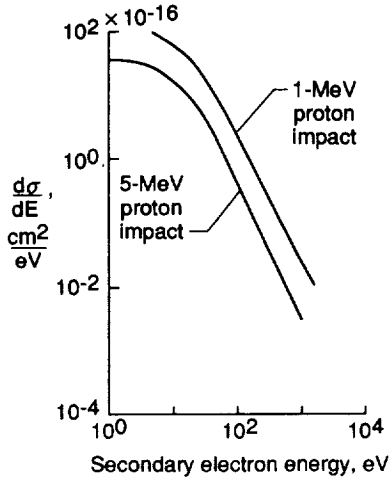

Figure 4. Secondary electron production spectra from proton impact with helium.

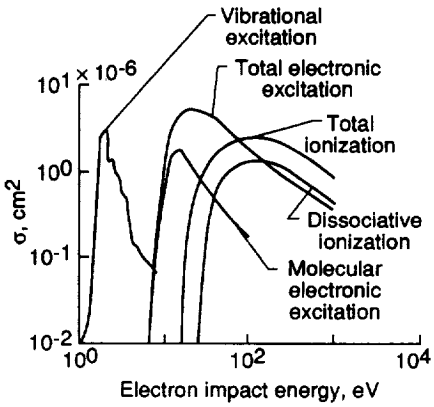

Figure 5. Electron impact cross section with N_2 molecules.

secondary electrons are broadly dispersed throughout the media giving a rather uniform distribution of ionization and excitation events.

The initiating events occur on the time scale of the passing ionizing particle ($\sim 10^{-14}$ sec). Even a free thermal target particle would drift less than 10^{-5} μm (0.1Å) in this time period. Clearly, diffusion and chemical reaction are precluded in this time period. The initiating events produce ions and free radicals within the media distributed in space according to the nature of the particle initiating the event. Whether the event is initiated by a neutral particle or passing ion, the secondary electrons ultimately dominate in producing the nascent chemical products. The source distribution (in space and energy) of the electrons is intimately connected to the initiating event and largely determines the initial distribution of ions and radicals (Rustgi et al., 1988). To a first approximation the distribution of ions and radicals is related to the average energy deposit first studied by Schaefer (1952) and extensively investigated by Katz and coworkers (for example, Katz et al., 1971).

The organic molecules of a living cell are suspended in water so that the radiolysis of water is one key to understanding mechanism of radiation injury. Without details we simply note that a principle product is the dissociation of H_2O into hydrogen and hydroxyl radicals (Casarett, 1968).

$$H_2O \rightarrow H + OH$$

Subsequent events depend on the density of such radicals and the other molecules present. At high power densities, peroxide and hydrogen formation

$$OH + OH \rightarrow H_2O_2$$

$$H + H \rightarrow H_2$$

are in competition with recombination

$$H + OH \rightarrow H_2O$$

In the presence of dissolved oxygen the peroxyl radical is formed as

$$H + O_2 \rightarrow HO_2$$

which cycles to form hydrogen peroxide

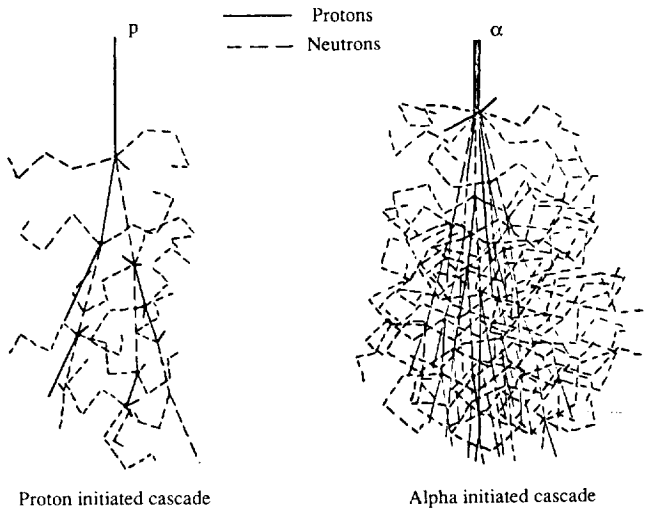

Figure 6. Cascade development in matter.

$$HO_2 + HO_2 \rightarrow O_2 + H_2O_2$$

The peroxides are highly active chemical (oxydizing) agents which are biologically damaging. The density of hydroxyl radicals and peroxides are undoubtedly related to damage to nearby organic molecules. Within the energy deposit are also organic molecules which may likewise be disassociated and form peroxyl radicals which may further form chemical reactions. Although we may not know specifically how a given structure within the DNA is altered it is easy to imagine that the degree of alteration of the DNA by either direct interaction or a chemical product is related to the local energy density associated with the initial event.

We will not attempt to describe the processes by which the DNA is damaged by the radicals and chemical agents described above but simply note that the direct reaction of these species with the organic molecules is a linear kinetic process. Furthermore, the enzyme repair of such damage is also expected to follow a linear kinetic description (Ngo et al., 1990). Even in spite of these facts, we would try linear kinetic modeling on the general principle of "keeping it simple" unless required to do otherwise according to experimental evidence. Nonlinear kinetics are of course important if sufficient energy is given to the cell in a sufficiently short time but such exposure levels are not assumed important to space radiation protection.

A SIMPLE LINEAR KINETIC SURVIVAL MODEL

Whether the DNA is altered by the direct interaction of the passing particle or chemical agents produced in the surrounding medium we may think in terms of chemical change at a specific site along the DNA chain which we term a lesion. Due to the complexity of the DNA molecule it is clear that many different types of lesions may occur and may exist along the DNA strand simultaneously. Such lesions are those we have termed the nascent cellular lesions (Wilson and Cucinotta, 1991). These nascent lesions are formed soon after the passage of the ionizing particle and are now dealt with by the slower cell repair processes (Ngo et al., 1990). Radiation injury to a DNA site is related to the probability of an initiating ionization/excitation event at or near the site and the probability that a chemical lesion results. The probability of the initiation is related to the absorption cross section and the probability of forming a lesion is related to chemical kinetics within the energy deposit and rates of diffusion. The lesion formation rates are proportional to the ionizing particle flux and

depend on particle type. If $n_0(0)$ is the number of cells present before irradiation then the cell kinetic equations (without repair) are given as

$$\dot{n}_0(t) = -kn_0(t) \tag{1}$$

$$\dot{n}_i(t) = k_i n_0(t) + \sum_{j=1}^{i-1} k_{i-j} n_j(t) - kn_i(t) \tag{2}$$

where $n_i(t)$ are the number of cells with i lesions. The k_i are rate coefficients (cross section times flux) for forming i lesions and depend on the spatial extent of the energy deposit (track structure). We expect for low LET radiation that $k_i \approx 0$ for $i > 1$ while high LET particles have significant contributions for $i > 1$. The nonlinear kinetic processes relate the distribution of energy deposit to lesion formation. Note that the conservation of cells requires

$$k = \sum_i k_i \tag{3}$$

The distribution of nascent lesions in the cell population after a time t is

$$n_0(t) = n_0 e^{-kt} \tag{4}$$

$$n_1(t) = n_0 k_1 t\, e^{-kt} \tag{5}$$

$$n_2(t) = n_0 \left[k_2 t + \frac{1}{2}(k_1 t)^2 \right] e^{-kt} \tag{6}$$

$$n_3(t) = n_0 \left[k_3 t + \frac{2}{2!} k_1 t k_2 t + \frac{1}{3!}(k_1 t)^3 \right] e^{-kt} \tag{7}$$

and similarly for higher order terms where $n_0 \equiv n_0(0)$. It is likely that these nascent lesions are chemical alterations yet to be stabilized by the cell repair processes.

If in subsequent reactions the DNA is restored to its original state then the cell has been repaired. Some altered status after repair is called misrepair and the cell undergoes clonogenic death (Casarett, 1968). We assume a simple form for the linear repair kinetics as

$$\dot{n}_0(t) = \sum_{i=1}^{\infty} \alpha_{ri} n_i(t) \tag{8}$$

$$\dot{n}_i(t) = -\alpha_i n_i(t) \tag{9}$$

where α_{ri} and α_i are repair rate coefficients. The balance of misrepaired cells are

$$\dot{n}_d(t) = \sum_{i=1}^{\infty} \alpha_{mi} n_i(t) \tag{10}$$

where α_{mi} is the misrepair rate coefficient. Conservation of number of cells requires $\alpha_i = \alpha_{ri} + \alpha_{mi}$. The subsequent repaired, unrepaired, and misrepaired states are given by

$$n_0(t) = n_0(0) + \sum_{i=1}^{\infty} n_i(0) \frac{\alpha_{ri}}{\alpha_i} \left(1 - e^{-\alpha_i t} \right) \tag{11}$$

$$n_i(t) = n_i(0) e^{-\alpha_i t} \tag{12}$$

$$n_d(t) = \sum_{i=1}^{\infty} n_i(0) \frac{\alpha_{mi}}{\alpha_i} \left(1 - e^{-\alpha_i t} \right) \tag{13}$$

where $n_0(0)$ and $n_i(0)$ represents in equations (11) through (13) and in subsequent equations the lesion distribution at the start of the repair period. After the repairs are complete ($\alpha_i t \gg 1$) the final populations are given as

$$n_0(\infty) = n_0(0) + \sum_{i=1}^{\infty} \frac{\alpha_{ri}}{\alpha_i} n_i(0) \tag{14}$$

$$n_d(\infty) = \sum_{i=1}^{\infty} \frac{\alpha_{mi}}{\alpha_i} n_i(0) \tag{15}$$

which are dependent on the initial distribution of lesions and the repair efficiencies. At 100 percent repair efficiency

$$n_0(\infty) = n_0(0) + \sum_{i=1}^{\infty} n_i(0) \equiv n_0 \tag{16}$$

so that the population is fully restored to its initial number n_0 prior to exposure. In practice, relatively efficient repair is found for $i < m_d$ with nearly complete misrepair for higher numbers of lesions ($i \geq m_d$). The final population is then

$$n_0(\infty) = n_0(0) + \sum_{i=1}^{m_d - 1} n_i(0) \tag{17}$$

Examination of $n_0(\infty)$ for a short γ-ray exposure period t with the aid of equations (4) to (7) yields

$$n_0(\infty) \approx n_0 \left[1 - \frac{1}{m_d!} (k_1 t)^{m_d} \right] \tag{18}$$

with $k_i = 0$ for $i > 1$. This solution shows typical sigmoid response at low dose. If however $k_{m_d} \neq 0$ as expected for HZE exposure then

$$n_0(\infty) \simeq n_0(1 - k_{m_d} t) \tag{19}$$

exhibiting a linear slope response with no shoulder. Clearly a broad range of solution is available as a function of radiation type (k_i) and the repair efficiencies.

The cellular repair mechanisms depend on the overall status of the cell chemistry. The chemical processes in the cell vary greatly throughout the cell cycle. For example, the cytoplasm viscosity is normally quite high and suddenly drops to near zero just before mitosis. Such shifts in physical properties are affected through the cell chemistry and reflects tremendous variability. More subtle are the changes prior to synthesis as well as throughout the synthesis phase. Such variations are clearly seen in different experimental protocols with the same cell line and radiation source. These considerations will be key to determination of the coefficients in the above kinetic equations.

Sigmoid Survival Curves

If any particle is capable of forming single lesions it is the photon. We further assume the photon to form only single lesions. The lesion distribution for a pulse of photons of duration t_r is then

$$n_0(t_r) = n_0 e^{-kt_r} \tag{20}$$

$$n_i(t_r) = n_0 \frac{1}{i!} (k_1 t_r)^i \, e^{-kt_r} \tag{21}$$

Allowing for complete repair subsequent to exposure yields

$$\frac{n_0(\infty)}{n_0} = 1 - \sum_{i=1}^{\infty} \frac{\alpha_{mi}}{\alpha_i} \frac{1}{i!} (k_1 t_r)^i \, e^{-kt_r} \tag{22}$$

The response is proportional to the exposure to the m_d power where m_d is the lowest i for which $\alpha_{mi} \neq 0$. Generally, there could be a small linear term present if $0 < \alpha_{m1}/\alpha_1 \ll 1$. Such a response would appear linear-quadratic at low exposure. Note that a linear term could also arise from $k_{m_d} > 0$ for γ-rays as well.

Exponential Survival Curves

The exposure with high energy iron ions is near exponential and would be accommodated if the $k_i \approx 0$ for all $i < m_d$. The lesion distribution would then be

$$n_0(t_r) = n_0 e^{-kt_r} \tag{23}$$

$$n_i(t_r) = 0 \tag{24}$$

$$n_{m_d}(t_r) = k_{m_d} t_r e^{-kt_r} \tag{25}$$

The survival is given as

$$\frac{n_0(\infty)}{n_0} = 1 - \frac{\alpha_{m1m_d}}{\alpha_{1m_d}} k_{m_d} t_r e^{-kt_r} - \frac{\alpha_{m2m_d}}{\alpha_{2m_d}} \frac{1}{2!} (k_{m_d} t_r)^2 e^{-kt_r} - \ldots \tag{26}$$

showing linear-quadratic dependence at low exposure. If the repair efficiency is zero for $i \geq m_d$ then the response is given as

$$\frac{n_0(\infty)}{n_0} = e^{-k_{m_d} t_r} \tag{27}$$

as is usually observed for iron beam exposures.

Discussion

In summarizing our results to this point, we have suggested that track structure effects and the associated fast nonlinear kinetic processes contribute to the source terms for nascent lesions within the cell DNA. That the subsequent repair kinetics are much slower and are represented by linear repair processes (Ngo et al., 1990). The sigmoid behavior in survival curves is related to repair efficiency and the exponential survival curves of HZE particles result from track structure effects for which multiple lesions are formed in a single ion passage. We now consider means of evaluating the kinetic parameters through relation to a track structure model and repair dependent experiments.

TRACK STRUCTURE MODEL

The cellular track model of Katz et al. (1971) attributes biological damage from energetic ions to the secondary electrons (delta rays) produced along the ion's path. The effects caused by energetic ions are correlated with those of gamma rays by assuming the response in sensitive sites near the ion's path is part of a larger system irradiated with gamma rays at the same dose. The response due to ion effects is then approximately related to the gamma-ray response and the delta-ray dose surrounding the ion's path. For a multitarget response with target number m, the inactivation of cells by gamma rays is assumed to follow a multitarget distribution reflecting the random accumulation of sublethal damage, with a radiosensitivity parameter D_o.

For the inactivation of cells by ions, two modes are identified: "ion-kill" which corresponds to intratrack effects and "gamma-kill" which corresponds to intertrack effects. Here, the ion-kill mode is unique to ions corresponding to single particle inactivation of cells described by the cross section σ. The inactivation cross section for a sensitive site whose response to radiation is ahistoric is determined as

$$\sigma = \int_0^\infty 2\pi r dr (1 - e^{-\overline{D}/D_0})^m \tag{28}$$

where $\overline{D}$ is the average dose at the sensitive site from the ion's delta rays. The evaluation of the cross section is separated by Katz et al. (1971) into a so-called grain-count regime, where inactivation occurs randomly along the path of the particle, and into the so-called track-width regime, where many inactivations occur and are said to be distributed like a "hairy-rope." In the grain-count regime, σ may be parameterized as

$$\sigma = \sigma_0 (1 - e^{-Z^{*2}/\kappa\beta^2})^m \tag{29}$$

where σ_0 is the plateau value of the cross section, the effective charge number is given by

$$Z^* = Z(1 - e^{-125\beta/Z^{2/3}}) \tag{30}$$

and κ is a parameter related to the radius of the sensitive site, a_0, by

$$D_0 a_0^2/\kappa \cong 2 \times 10^{-7} \text{ erg/cm} \tag{31}$$

The transition from the grain-count regime to the track-width regime is observed to take place at a value of $Z^{*2}/\kappa\beta^2$ of about 4 at lower values we are in the grain-count regime and at higher values the track-width regime.

The fraction of the cells damaged in the ion-kill mode is $P = \sigma/\sigma_0$ and note that in the track-width regime $\sigma > \sigma_0$ and it is assumed that $P = 1$. The track model assumes that a fraction of the ion's dose, $(1 - P)$, acts cumulatively with that for other particles to inactivate cells in the gamma-kill mode. The surviving fraction of a cellular population $n_0(\infty)$, whose response parameters are m, D_0, and κ or a_0 after irradiation by a fluence of particles F, is then written

$$\frac{n_0(\infty)}{n_0} = \pi_i \times \pi_\gamma \tag{32}$$

where

$$\pi_i = e^{-\sigma F} \tag{33}$$

is the ion-kill survival probability and

$$\pi_\gamma = 1 - \left(1 - e^{-D_\gamma/D_0}\right)^m \tag{34}$$

is the gamma-kill survival probability. The gamma-kill dose fraction is

$$D_\gamma = (1 - P)D \tag{35}$$

where D is the absorbed dose. Note this division into ion-kill and gamma-kill also divides our track into regions where the fast nonlinear kinetics are expected to dominate (ion-kill) and a region where the fast linear kinetics are expected to be more important (gamma-kill).

The RBE at a specific survival level is given by

$$\text{RBE} = D_x/D \tag{36}$$

where

$$D_x = -D_0 \ln\left\{1 - \left[1 - n_0(\infty)/n_0\right]^{1/m}\right\} \tag{37}$$

is the x-ray dose at which this level is obtained. Equations (28) through (37) represent the cellular track model for monoenergetic particles. We must now consider the relationship of the kinetic model to the Katz model.

Physics and Kinetics of Cell Injury

The Katz model is formulated on the basis of physical arguments about track structure, geometric arrangement of sensitive (chemical bond) sites, the size of the cell nucleus, and energy thresholds for changes in the cell molecules. In practice, the Katz parameters $(m, D_0, \sigma_0, \kappa)$ are determined from biological experiments for a given cell system and experimental protocol. The degree to which cell repair is reflected in the final parameters is uncertain, but the effects of differing experimental protocols on the Katz parameters are well known and in someway reflect repair mechanisms. We will attempt to better define the relationship of repair to the Katz model parameters within the context of the present repair kinetic model.

In the Katz model, it is assumed that electromagnetic radiations form single lesions with an efficiency related to D_0 and generally more than one lesion ($m_d \geq 2$) is required to express the biological effect (cell death in the present case). We assume that stationary G_1 phase cells show near complete repair of lesion multiples less than m_d. If the cells are irradiated with γ-rays in stationary G_1 and are held in this phase until repair is complete, then the surviving population is found to be

$$n_0(\infty) \approx n_0(t_r) + \sum_{i=1}^{m_d-1} n_i(t_r) \tag{38}$$

assuming maximum repair in stationary G_1 (i.e., $\frac{\alpha_{r_i}}{\alpha_i} \approx 1$ for $i < m_d$). Equation (38) allows us to relate the k_i coefficients to the corresponding Katz parameters of equations (28) to (35) as applied to the appropriate experimental protocol (namely, G_1 exposure followed by complete G_1 repair). In the kinetic model, n_0 is the initial number of G_1 cells, and equation (38) is rewritten as

$$\frac{n_0(\infty)}{n_0} \approx e^{-kt_r} + \sum_{i=1}^{m_d-1} k_i t_r e^{-kt_r} + \frac{1}{2!} k_1 t_r \sum_{i=1}^{m_d-1} k_i t_r e^{-kt_r} + \frac{1}{3!}(k_1 t_r)^2 \sum_{i=1}^{m_d-2} k_i t_r e^{-kt_r} + \ldots \tag{39}$$

According to the Katz model, a $m_d = 3$ system has a γ-ray response given by

$$\frac{n_0(\infty)}{n_0} \approx 1 - \left(1 - e^{-D_\gamma/D_0}\right)^3 \approx 1 - \left(\frac{D_\gamma}{D_0}\right)^3 \tag{40}$$

which is matched to equation (39) if

$$k_1 t_r \cong 6^{\frac{1}{3}} D_\gamma / D_0 \tag{41}$$

$$k_m t_r \approx 0 \quad (m > 1) \tag{42}$$

as is appropriate for γ-rays. Similarly, the remaining terms in equation (39) can be determined from the remaining Katz terms by noting for strictly ion kill kinetics

$$k_3 t_r \cong \sigma F \tag{43}$$

$$k_2 t_r \cong 0 \tag{44}$$

Requiring k_2 to be zero results from our matching of equation (39) at low dose. There may be nonzero values of k_2 but they cannot be strictly determined in the present form of Katz's theory. Although the k_i's may reflect both physical and chemical processes because of their empirical nature, we assume here that they are most clearly identified with the physical processes discussed by Katz. We now examine means by which repair rates can be estimated at least for some experimental cell systems.

Three-target Repair/Misrepair Systems

The above can be applied to an approximate three-target system as

$$\frac{n_0(\infty)}{n_0} \approx \left[1 + \frac{\alpha_{r_1}}{\alpha_1} 6^{\frac{1}{3}} \frac{D_\gamma}{D_0} + \frac{\alpha_{r_2}}{\alpha_2} \frac{6^{\frac{2}{3}}}{2} \frac{D_\gamma^2}{D_0^2}\right] e^{-\sigma F - 6^{\frac{1}{3}} D_\gamma / D_0} \tag{45}$$

where D_γ, D_0, and σF are related to the usual Katz model for $m_d = 3$ and $\frac{\alpha_{r_1}}{\alpha_1}, \frac{\alpha_{r_2}}{\alpha_2}$ are the repair ratios for the once hit and twice-hit cells. Presumably, $\frac{\alpha_{r_1}}{\alpha_1} > \frac{\alpha_{r_2}}{\alpha_2}$. We take

$$\frac{\alpha_{r_2}}{\alpha_2} = \left(\frac{\alpha_{r_1}}{\alpha_1}\right)^p \tag{46}$$

in the present analysis and expect p to be 2 or greater. In the limit of vanishing dose where RBE is presumably maximum

$$\mathrm{RBE}_m \approx 1 - \frac{\sigma}{\sigma_0} + 6^{-\frac{1}{3}} D_0 \frac{\alpha_1 \sigma}{\alpha_{m_1} L} \tag{47}$$

which is unbound for small α_{m1}. The RBE in the Katz model is found to increase with ion dose as $D^{-1+1/m}$ (Cucinotta et al. 1991, Katz and Cucinotta 1991) so that no maximum is achieved. A similar dependence on dose is found here at higher exposure levels than assumed in equation (47), however, misrepair prevents a one-to-one correspondence especially at low dose where a maximum RBE is achieved in the kinetics model for $\alpha_{m_1} > 0$.

APPLICATION TO CELL SURVIVAL

The experiments of Yang et al. (1989) have utilized contact stabilized mouse cells C3H10T1/2 in the stationary G_1 phase. In one set of experiments, the cells were held in the G_1 phase for 24 hours before separation and introduction into a nutrient medium to stimulate growth (delayed plating). A second series of cells was immediately plated and thus greatly altered the cell kinetics by progression towards the synthesis cycle (S phase) soon after exposure. It is well known (Sinclair, 1968) that the early G_1 phase is efficient in cell repair while the early S phase is mistake prone (Radman et al., 1981). We assume the stationary G_1 phase repair ratio $\frac{\alpha_{r1}}{\alpha_1}$ is near maximum, while the accident-prone early S phase has a significant rate of misrepair. Furthermore, cell survival of the mouse cell is shown by Katz to be a three-target system, and even higher rates of misrepair are expected from the doubly injured cell ($p \gg 2$), especially later in the cell cycle.

The Katz parameters (see table 1) for the delayed experiments (Waligorski et al., 1987) are used directly to estimate $\sigma F, D_0, D_\gamma$ with assumed $\frac{\alpha_r}{\alpha} = 1$ and provides a good fit, as expected, to Yang et al.'s delayed plating data. Good agreement is found for the immediately plated cells by taking $p = 6$ and $\frac{\alpha_{r_1}}{\alpha_1} = 0.7$ (for the exponential population). The results are shown in figure 7. The figure is arranged in the order of increasing LET, and the sigmoid behavior associated with multitarget phenomena is apparent for the lighter ions. The sigmoid behavior disappears at higher LET as the repair processes become less effective and the ion-kill mechanism of Katz dominates.

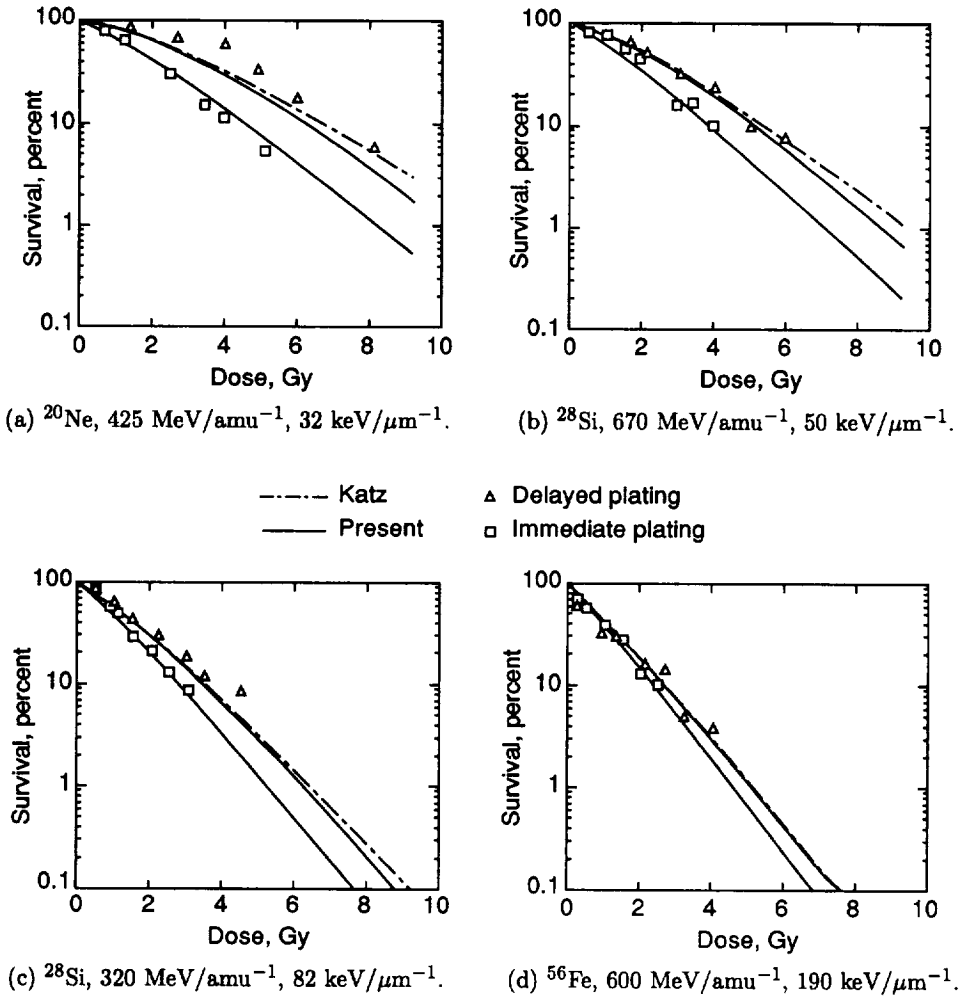

(a) ^{20}Ne, 425 MeV/amu^{-1}, 32 keV/μm^{-1}.

(b) ^{28}Si, 670 MeV/amu^{-1}, 50 keV/μm^{-1}.

(c) ^{28}Si, 320 MeV/amu^{-1}, 82 keV/μm^{-1}.

(d) ^{56}Fe, 600 MeV/amu^{-1}, 190 keV/μm^{-1}.

Figure 7. Cell survival of C3H10T 1/2 for delayed plating (Δ) and immediate plating (□). The dash-dot curves are Katz model values while the present model values are the full curves.

Comparisons of calculated and measured RBE values for several ions are shown in table 2 at survival levels of 10 percent and 50 percent for immediate plating conditions. The agreement with experiment is very good except for the U ion. Here, we have not taken track-width effects in the thin down region into account. The maximum RBE value given by equation (47) with $\alpha_{ri}/\alpha_i = 0.7$ is also shown in table 2. We note that for the delayed plating experiments, no maximum RBE is predicted in the kinetic model (assumed $\alpha_{m1} = 0$), as well as in the Katz model (Katz and Cucinotta, 1991).

TABLE 1. KATZ PARAMETERS FOR CELL SURVIVAL USED IN THE PRESENT TRACK STRUCTURE REPAIR/MISREPAIR MODEL

	σ_0, cm^2	κ	m	D_0, Gy
C3H10T 1/2	5×10^{-7}	750	3	2.8

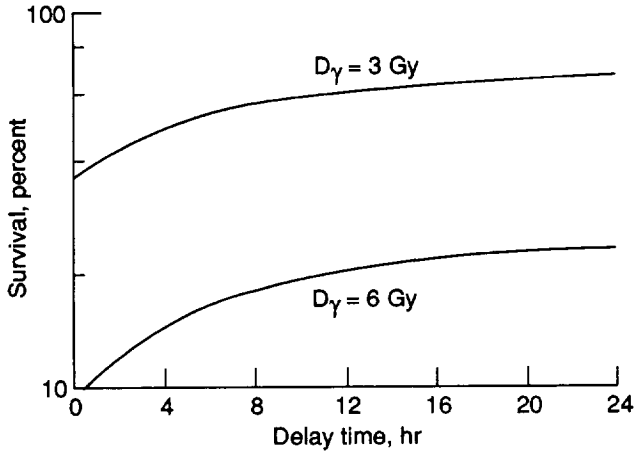

Figure 8. Percent survival at two exposure levels as a function of G_1 delay time before plating.

TABLE 2. RBE FOR SURVIVAL OF C3H10T 1/2 CELLS (IMMEDIATE PLATING)

		10%	50%	Maximum
Radiation	LET*	Experiment (Theory)	Experiment (Theory)	Theory
x-rays		1.00 (1.00)	1.00 (1.00)	1.00
C-12	10	1.00 (1.03)	1.00 (1.02)	1.10
Ne-20	32	1.50 (1.29)	1.56 (1.38)	1.71
Si-28	50	1.50 (1.52)	1.67 (1.67)	2.28
Si-28	82	2.23 (2.10)	3.00 (2.51)	3.73
Ar-40	140	2.30 (2.60)	3.00 (3.15)	5.00
Fe-56	192	2.20 (2.50)	3.10 (3.08)	4.87
Fe-56	286	2.00 (2.35)	3.00 (2.99)	4.68
Fe-56	475	1.62 (1.65)	2.72 (2.11)	3.31
U-238	1860	0.88 (0.43)	1.20 (0.55)	0.86

*LET in units of keV/μm

Although the present results are encouraging, there is a fuller range of protraction experiments to which the model is to be compared. Furthermore, other biological endpoints must yet be added and further tested against experimental observation.

Repair Rate Dependent X-ray Experiments

Another useful experiment is the exposure of a stationary G_1 population and to allow G_1 phase repair to proceed for a fixed time t followed by plating in which the full cell cycle is promoted. The initially injured cell population after exposure described by $n_i(t_r)$ is given by equations (4) to (7). The G_1 repair phase is described by

$$n_0(t) = n_0(t_r) + \sum_{i=1}^{m_d-1} \left(\frac{\alpha_{r_i}}{\alpha_i}\right) n_i(t_r) \left(1 - e^{-\alpha_i t}\right) \tag{48}$$

and

$$n_i(t) = n_i(t_r) e^{-\alpha_i t} \tag{49}$$

If after a time t the cells are placed into a normal cell cycle the exponential phase repair rates are quite different and the system proceeds at the repair rates found by Wilson and Cucinotta (1991) as

$$n_0(\infty) = n_0(t_r) + \sum_{i=1}^{m_d-1} \left(\frac{\alpha_{r_i}}{\alpha_i}\right) n_i(t_r) \left(1 - e^{-\alpha_i t}\right) + \sum_{i=1}^{m_d-1} \left(\frac{\alpha'_{r_i}}{\alpha'_i}\right) n_i(t_r)\, e^{-\alpha_i t} \tag{50}$$

where t remains as the G_1 repair period and α'_{r_i} and α'_i are the repair rate coefficients for an exponential population. Results are shown in figure 8 as a function of G_1 delay for two x-ray exposure levels of 3 and 6 Gy.

Another approach to study G_1 repair rates is to use fractionated exposures of a G_1 population. The initial exposure followed by a G_1 repair period of length t results in a cell population after repair of

$$n_0(t) = n_0(t_r) + \sum_{i=1}^{m_d-1} \left(\frac{\alpha_{r_i}}{\alpha_i}\right) n_i(t_r) \left(1 - e^{-\alpha_i t}\right) \tag{51}$$

and

$$n_i(t) = n_i(t_r) e^{-\alpha_i t} \tag{52}$$

A subsequent second exposure of equal duration t_r results in a new population

$$n'_0(t_r) = n_0(t)\, e^{-kt_r} \tag{53}$$

$$n'_1(t_r) = n_1(t)\, e^{-kt_r} + k_1\, t_r\, n_0(t)\, e^{-kt_r} \tag{54}$$

$$n'_2(t_r) = n_2(t)\, e^{-kt_r} + n_1(t)\, k_1\, t_r\, e^{-kt_r} + \frac{1}{2}\, n_0(t)\, k_1^2\, t_r^2\, e^{-kt_r} \tag{55}$$

which if plated immediately after exposure yields

$$n'_0(\infty) = n'_0(t_r) + \sum_{i=1}^{m_d-1} \left(\frac{\alpha'_{r_i}}{\alpha_i}\right) n'_i(t_r) \tag{56}$$

These results are compared to the variable repair and fractionated exposure experiments of Yang et al. (1989) in figure 9. The agreement is excellent.

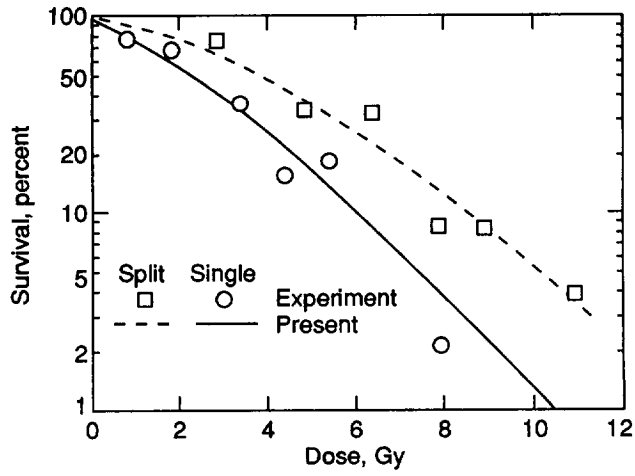

Figure 9. Comparison of present theory with Yang's experiments for single and fractionated exposure.

Target Fragments in Proton Induced Kinetics

The target fragmentation fields are found in closed form in terms of the collision density (Wilson, 1977), because the fragment ions are of relatively low energy. Away from any interfaces, the target fields are in local equilibrium and may be written as

$$\phi_\alpha(x, E_\alpha; E_j) = \frac{1}{S_\alpha(E_\alpha)} \int_{E_\alpha}^{\infty} \frac{d\Sigma_{\alpha j}(E', E_j)}{dE'} \phi_j(x, E_j) dE' \tag{57}$$

where the subscript α labels the target fragment type, $S_\alpha(E)$ the stopping power, and E_α and E_j are in units of MeV.

The particle fields of the projectiles and target fragments determine the level and type of radiation damage for the endpoint of interest. The relationship between the fields and the cellular response is now considered within the Katz cellular track model.

The ion-kill term now contains a projectile term (Cucinotta et al., 1991b) as well as a target fragment term as

$$(\sigma F) = \sigma_j(E_j)\phi_j(x, E_j) + \sum_\alpha \int_0^\infty dE_\alpha \phi_\alpha(x, E_\alpha; E_j)\sigma_\alpha(E_\alpha) \tag{58}$$

while the corresponding gamma-kill dose becomes

$$D_\gamma = [1 - P_j(E_j)]S_j(E_j)\phi_j(x, E_j) + \sum_\alpha \int_0^\infty dE_\alpha [1 - P_\alpha(E_\alpha)]S_\alpha(E_\alpha)\phi_\alpha(x, E_\alpha; E_j) \tag{59}$$

Use of equation (57) allows one to define an effective cross section as

$$\sigma_j^*(E_j) = \sigma_j(E_j) + \sum_\alpha \int_0^\infty dE_\alpha \frac{\sigma_\alpha(E_\alpha)}{S_\alpha(E_\alpha)} \int_{E_\alpha}^\infty dE' \frac{d\Sigma_{\alpha j}(E', E_j)}{dE'} \tag{60}$$

The first term of equation (60) is caused by the direct ionization of the media by the passing ion of type j. The second term results from target fragments produced in the media.

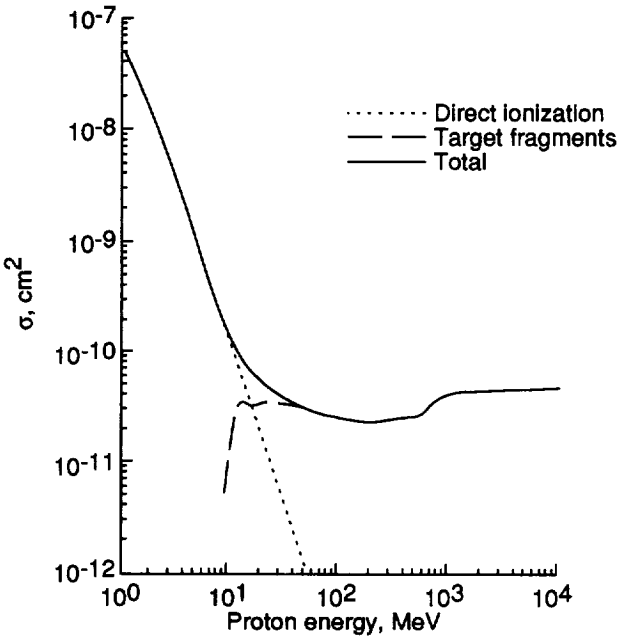

Figure 10. Katz cross section for protons in C3H10T 1/2 cells.

The Katz (Waligorski et al., 1987) cellular parameters for survival of C3H10T1/2 fit to the experiments of Yang et al. (1985) as given in table 1 are used to evaluate target fragment contributions according to equations (59) and (60). General agreement with the measured RBE values (Waligorski et al., 1987) was found using these parameter sets. The single-particle inactivation cross section neglecting target fragmentation of equation (60) is shown in figure 10 for cell death as a function of the energy, MeV, of the passing proton. The target fragmentation contribution [second term of equation (60)] has been evaluated and also shown in figure 10. For protons, the effect of the target fragments (dashed line, the second term of equation (60)) dominates over the proton direct ionization (dotted line) at high energy. For high-LET particles (low energy), the direct ionization dominates and target fragmentation effects become negligible. The effects of target fragments on the gamma-kill dose equation (59) are small (Cucinotta et al., 1991b) and are neglected here. The effective cross section is now used to study the repair capability of the cell for target fragment induced lesions. We have calculated the immediate and delayed plating response including target fragment contributions and compare these with results in which target fragments are neglected (see figure 11).

Results for 10 MeV proton exposures are shown in figure 11a. The response curves are characteristic of x-ray exposures and target fragments play a small role at this energy. Exposures at 50 MeV and 100 MeV clearly display target fragment effects (figs. 11b and 11c) but are beyond our ability to measure in biological experiments. Target fragment effects are quite large at 1,000 MeV and show in figure 11d clearly a reduced capability of the cell to repair fragment induced lesions. When target fragments are neglected the response curves are nearly those expected for x-ray exposures.

Remarks

The multilesion track structure model described herein agrees well with the available experimental data for C3H10T 1/2 cells. The lack of repair capability of the cell for target fragment induced damage by high energy protons is predicted by the model. We must await further experiments to confirm these predictions.

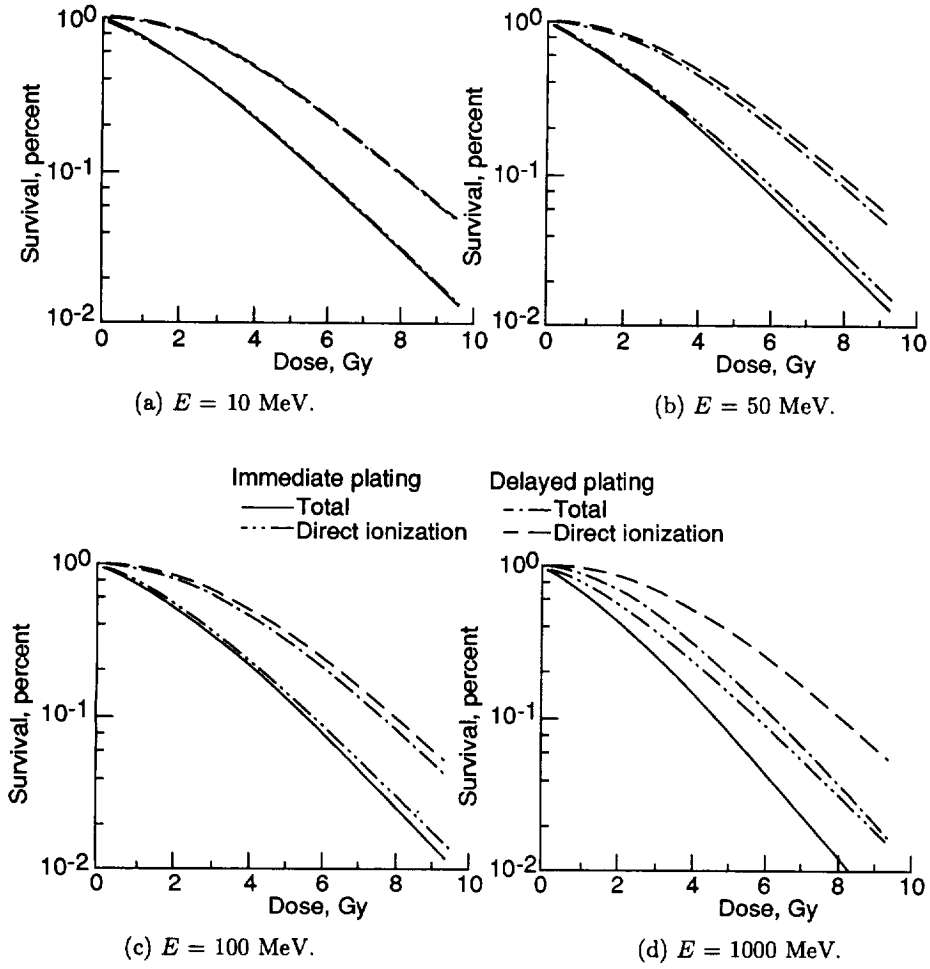

(a) $E = 10$ MeV. (b) $E = 50$ MeV.

(c) $E = 100$ MeV. (d) $E = 1000$ MeV.

Figure 11. Target fragmentation effects on repair processes in proton exposures.

CELL KINETIC EFFECTS ON RBE

Radiation exposure limits and the associated biological risks are mainly estimated from human exposures at the two nuclear weapon sites of WWII and were predominately due to γ-rays (BEIRV, 1990) although the neutron component is still uncertain. The quality factor Q is defined as an extrapolation factor for risk estimation for radiations of different quality and is a judgment from estimates of RBE_m as the low dose limit for selected biological endpoints (ICRU, 1986; Sinclair, 1985). It is assumed that RBE_m is dose rate independent and is achieved in controlled laboratory experiments usually with single exposure of the biological specimens. Cell cultures are playing an increasing role in determining RBE_m since the large populations required for low dose response is more easily achieved. An added advantage of cell culture studies is that the role of the effects of radiation quality may be better understood (Katz and Cucinotta, 1991) and the role of cell kinetics can be studied more directly in these simpler biological systems (Yang, et al., 1989). The limitation of the cell radiation studies is that the relationship of *in vitro* response to *in vivo* response is not fully understood. In the present section we use a simple kinetic model to shed some light on the use of cell culture derived RBE's and their possible implication for tissue systems within an organism.

Cell Kinetics

Ionizing radiation interacts with matter through the formation of radicals ultimately producing what we call the nascent lesions. These highly active chemical species produced within the cell may leave permanent structural change (misrepair) or restore the cell (repair) to its initial state. If these structural changes occur within the DNA then subsequent generations may exhibit new characteristics or the cell may be unable to undergo cell division for which death of the cell occurs.

There are many ways in which the DNA could be changed to cause cell death but only a few specific changes are allowed to reach other biological endpoints (Goodhead, 1985). Herein, we treat only those lesions which lead to cell death and write kinetic equations (Wilson and Cucinotta, 1991) for the time development of populations $n_i(t)$ with i-fold lesions as

$$\dot{n}_0(t) = \sum_{i=1}^{\infty} \alpha_{r_i} n_i(t) - k n_0(t) \tag{61}$$

$$\dot{n}_i(t) = \sum_{j=0}^{i-1} k_{i-j} n_j(t) - k n_i(t) - \alpha_i n_i(t) \tag{62}$$

$$\dot{n}_d(t) = \sum_{i=1}^{\infty} \alpha_{m_i} n_i(t) \tag{63}$$

where the k_i are proportional to the charged particle flux (primary and secondary), α_{r_i} are the repair rates, α_{m_i} are the misrepair rates, and $n_d(t)$ is the population of misrepaired cells. Conservation of cells within a given cell cycle requires $k = k_1 + k_2 + \ldots$ and $\alpha_i = \alpha_{r_i} + \alpha_{m_i}$. The ratio $\alpha_{r_i}\alpha_i^{-1}$ is the kinetic repair efficiency.

The k_i kinetic coefficients are related to the Katz model for the highly repair efficient stationary G_1 phase cells as

$$k_1 = (m_d!)^{\frac{1}{m_d}} \dot{D}_\gamma / D_0 \tag{64}$$

$$k_{m_d} = \sigma\phi \tag{65}$$

where all other k_i's are taken as zero and the remaining quantities are all given by Katz as

$$\dot{D}_\gamma = \left(1 - \frac{\sigma}{\sigma_0}\right) L\phi \tag{66}$$

where ϕ is the local charged particle flux (primary and secondary), L is their corresponding LET, σ is approximated using the Katz model, equations (29) to (31).

The repair coefficients are found to be cell phase dependent and the stationary G_1-phase repair efficiencies are near maximum for $i < m_d$ and near zero otherwise. The exponential population showed relatively high single lesion repair efficiency and much lower multiple lesion repair efficiencies (see table 3) in analyzing the repair dependent experiments of Yang, et al. (1989). As examples, the G_1 repair enhanced exposures (delayed plating) and exponential

TABLE 3. SURVIVAL REPAIR RATES (h^{-1}) AND REPAIR EFFICIENCIES

	G_1 Phase			Exponential Phase		
i	1	2	$> m$	1	2	$> m$
α_i	.25	.125	$< .08$	.25	.125	$< .08$
$\alpha_{r_i}\alpha_i^{-1}$	$> .97$	$> .84$	~ 0	.7	.118	~ 0

phase repair exposures are compared to the present results in figure 7 for various ions (Wilson and Cucinotta, 1991) and with x-ray fractionated exposures (Wilson, Cucinotta, and Shinn, 1991) in figure 8. We will use this model to study the functional dependence of RBE at low total dose for G_1 phase and exponential phase repair processes.

Low Dose Rate Exposures

We consider now a special solution of equations (61) to (63) for an exposure field with a low constant dose rate ($\alpha_i \gg k_j$ for all i, j). At low dose rates the populations of cells with lesions can be approximated as

$$n_1(t) \simeq k_1 n_0(t)/\alpha_1 \tag{67}$$

$$n_2(t) \simeq k_1^2 n_0(t)/\alpha_1\alpha_2 \tag{68}$$

$$n_3(t) \simeq (k_1^3/\alpha_1\alpha_2\alpha_3 + k_3/\alpha_3) n_0(t) \tag{69}$$

In the case of low total exposure $n_0(t)$ may be taken as constant and the accumulation of misrepaired cells is written as

$$\frac{n_m(t)}{n_0} \simeq \frac{\alpha_{m_1}}{\alpha_1} 6^{\frac{1}{3}} \frac{(1-P)D}{D_0} + \frac{\alpha_{m_2}}{\alpha_2} 6^{\frac{2}{3}} \frac{(1-P)^2 \dot{D} D}{D_0^2 \alpha_1} + \frac{\alpha_{m_3}}{\alpha_3} 6 \frac{(1-P)^3 \dot{D}^2 D}{D_0^3 \alpha_1 \alpha_2} + \frac{\alpha_{m_3}}{\alpha_3} \frac{\sigma}{L} D \tag{70}$$

where $\dot{D}$ is the dose rate and $P = \sigma/\sigma_0$. In the case of an exponential population $\frac{\alpha_{m_1}}{\alpha_1} \simeq 0.3$ so that the first term is always dominant over the second and third term for very low dose rate exposures ($\dot{D}\alpha_i^{-1} \ll D_0$). The RBE is found to be

$$\mathrm{RBE}_m = 1 - P + 6^{-\frac{1}{3}} \frac{\alpha_{m_3}}{\alpha_3} \frac{\alpha_1}{\alpha_{m_1}} \frac{\sigma}{L} D_0 \tag{71}$$

as was found for our earlier result (Wilson and Cucinotta, 1991). If the repair efficiency of G_1 phase is highly efficient $\left(\frac{\alpha_{m_1}}{\alpha_1} \ll \frac{\dot{D}}{\alpha_i D_0}\right)$ then the higher order terms of equation (70) cannot be ignored in determining RBE for which there are important dose rate dependent factors whenever $\dot{D} \gg \alpha_i D_0 \approx 0.01$ Gy min^{-1}. At much lower dose rates ($\dot{D} \ll 0.01 \frac{\alpha_{m_1}}{\alpha_1}$ Gy min^{-1}.) then the RBE_m given by equation (71) is obtained. A parameter study using the data in figure 7 shows $\frac{\alpha_{m_1}}{\alpha_1} < 0.03$ corresponding to 97 percent repair efficiency as noted in table 3. Taking this as the lower limit on G_1 repair efficiency the dose rate dependent low-dose limit of RBE is shown in figure 12. Although the exponential population RBE_m is easily achieved for all the ions shown in figure 12, the G_1 population RBE shows a strong dose rate dependence with the RBE_m reached at effectively zero dose rate. Clearly RBE_m will be difficult to measure experimentally.

Results and Discussion

Values of RBE_m are shown for the exponential population in figure 13 and table 2 according to the parameters in tables 1 and 3. Also shown in table 2 are RBE values measured by Yang, et al. at two exposure levels (corresponding to 10 and 50 percent survival levels). It might be surmised that a slight increase in repair efficiency for the exponential population may be appropriate according to table 2. The RBE for ^{4}He ions (Bettega, et al., 1990) shown as the single datum in figure 13 was measured at 0.01 Gy exposure. A 10 percent increase in $\alpha_{m_1}\alpha_1^{-1}$ would bring the theory and the ^{4}He datum into agreement. There are no low dose and low

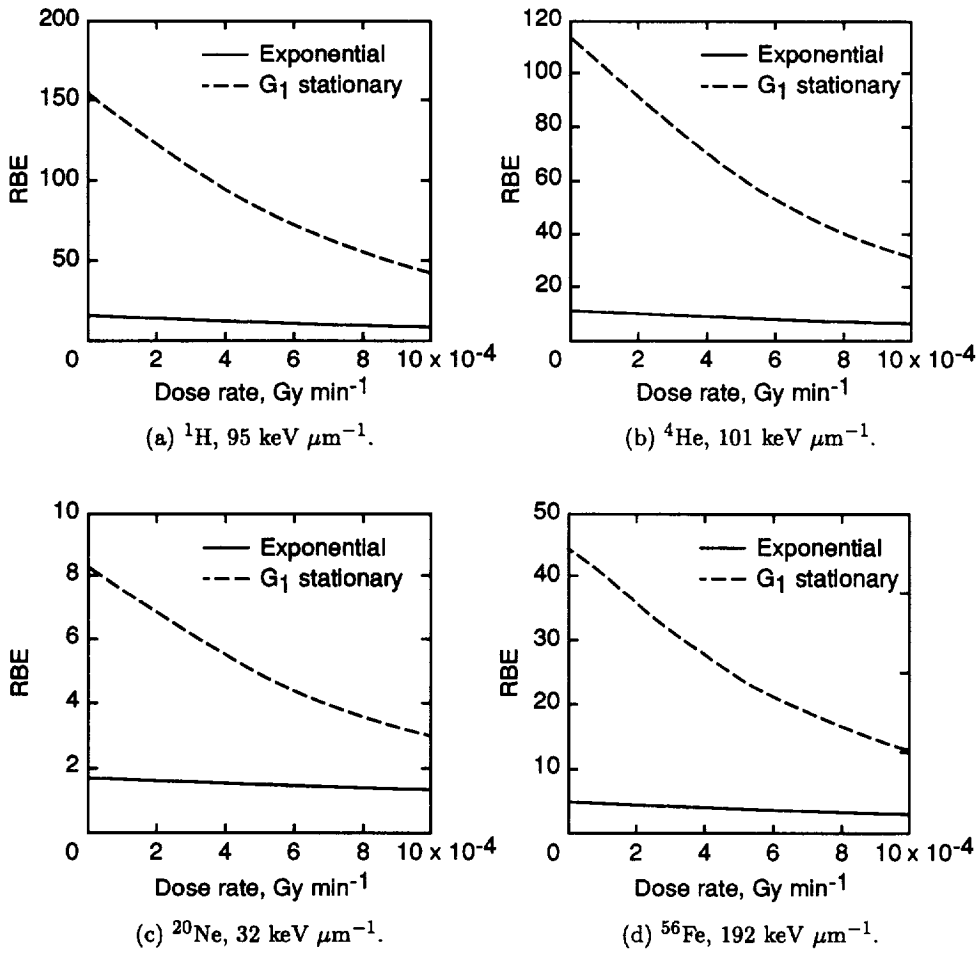

(a) ^{1}H, 95 keV μm^{-1}. (b) ^{4}He, 101 keV μm^{-1}.

(c) ^{20}Ne, 32 keV μm^{-1}. (d) ^{56}Fe, 192 keV μm^{-1}.

Figure 12. Predicted RBE for G_1 stationary and exponential population as a function of dose rate for various ion types.

dose rate measurements with which to make comparison for the G_1 population. Values greatly in excess of those given for the exponential population are expected. The low dose rate RBE measurements would be helpful in establishing the G_1 phase repair efficiencies.

Considering that highly differentiated tissues consist mainly of G_1 phase cells at any instant of time one might argue that the relevant RBE's for the mouse would be the stationary G_1 phase values which have not yet been measured and are difficult to estimate from current G_1 phase studies. The exponential phase RBE_m then appears as a lower limit on the relevant RBE values. Clearly the relevance of RBE_m of the exponential population to the mouse cannot be adequately resolved until the relationship of cell culture experiments to tissue response is better understood.

GENERALIZED LINEAR KINETIC MODEL

We assume at low total dose (<10 Gy) that cell injury is through damage on specific loci along the DNA strands and such loci are related to some characteristic of the cell. The nascent lesions are assumed to be chemically active species which directly involve the locus of interest. We label the loci as l and the number of lesions within the loci as i. Each locus will

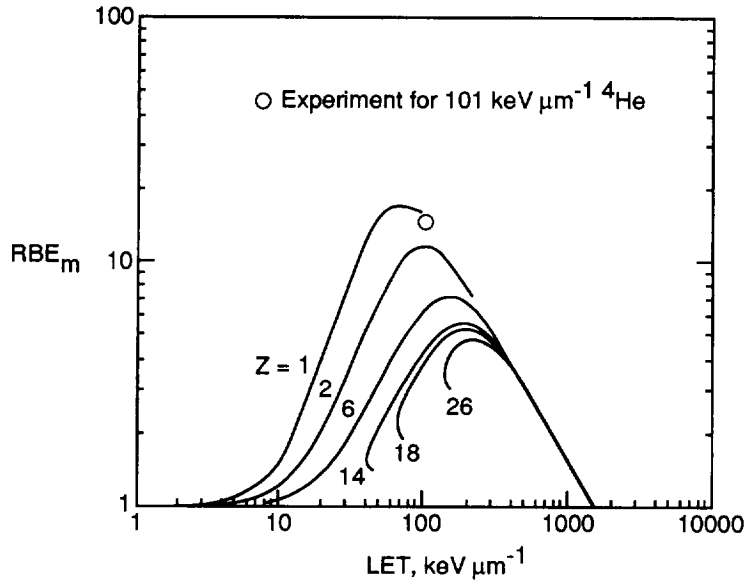

Figure 13. RBE_m for cell survival of a C3H10T 1/2 exponential population. The (○) is the value measured by Bettega, et al. (1990) for low energy ^{4}He ions at 0.01 Gy.

have lesion generation rates and repair rates similar to our multilesion model discussed in the previous sections. The initial uninjured population $n_0(0)$ then develops in time as

$$\dot{n}_0(t) = \sum_{li} \alpha_{rli}\, n_{li}(t) - k n_0(t) \tag{72}$$

where $n_{li}(t)$ is the number of cells with one loci l damaged with i lesions and α_{rli} is the corresponding repair rate coefficient and k is the rate at which damage is induced in the population. The α_{rli} represent the rates associated with a complex series of events resulting in the final repair of the locus. We assume a corresponding misrepair rate coefficient α_{mli} for which the highly chemically active species (radicals) have been stabilized but the corresponding locus is left in a misrepaired state

$$\dot{n}_l(t) = \sum_i \alpha_{mli} n_{li}(t) + \sum \alpha_{rl'i'} n_{ll'i'}(t) - k n_l(t) \tag{73}$$

and results in a permanent change in the state of the cell. The number of cells with l, i satisfy similar equations

$$\dot{n}_{li}(t) = \sum_{l'i'} \alpha_{rl'i'} n_{lil'i'}(t) + k_{li} n_0(t) + \sum_{j=1}^{i-1} k_{li-j} n_{lj}(t) - k n_{li}(t) - \alpha_{li} n_{li}(t) \tag{74}$$

where the collision induced lesion rate coefficients satisfy

$$k = \sum_{li} k_{li} \tag{75}$$

with

$$\alpha_{li} = \alpha_{rli} + \alpha_{mli} \tag{76}$$

and $n_{lil'i'}(t)$ are the cells with lesions at two loci and similar rate equations.

There are many ways in which a cell can be injured leading to clonogenic death and only a few specific changes can occur for the cell to transmit altered character to subsequent generations. If we sum over those loci associated with cell death and other specific target loci associated with altered characteristics then the above equations undergo great simplification. First we define

$$k_{di} = \sum_{l\epsilon d} k_{li} \tag{77}$$

where $l\epsilon d$ denotes all l which are associated with cell death. Then the total rate of induced injury is

$$k_i = k_{di} + \sum_{l\epsilon s} k_{li} \tag{78}$$

where $l\epsilon s$ are associated with injury at loci associated with survivability. The $l\epsilon s$ would include neoplastic transformations or mutagenic changes in the DNA. The repair rates are similarly defined as

$$\alpha_{di} = \sum_{l\epsilon d} \alpha_{li} / \sum_{l\epsilon d} 1^l \tag{79}$$

We assume all of the individual rates k_{li} and α_{li} are of similar magnitude so that the equations may be rewritten in terms of sums over $l\epsilon d$. Equation (72) is then

$$\dot{n}_0(t) = \sum_i \alpha_{rdi} n_{di}(t) + \sum_{l,i} \alpha_{rli} n_{li}(t) - k n_0(t) \tag{80}$$

where the second sum is over all l which do not contribute to d. Similarly equation (73) becomes

$$\dot{n}_d(t) = \sum_i \alpha_{mdi} n_{di}(t) + \sum_i \alpha_{li} n_{lid}(t) + \sum_{i'} \alpha_{mdi'} n_{ldi'}(t) - k_s n_d(t) \tag{81}$$

and

$$\dot{n}_l(t) = \sum_i \alpha_{mli} n_{li}(t) + \sum_{i'} \alpha_{rdi'} n_{ldi'}(t) - k_d n_l(t) \tag{82}$$

with equation (74) given by

$$\dot{n}_{di}(t) = \sum_{l'i'} \alpha_{rl'i'} n_{l'i'di}(t) + k_{di} n_0(t) + \sum_{j=1}^{i-1} k_{di-j} n_{dj}(t) - k n_{di}(t) - \alpha_{di} n_{di}(t) \tag{83}$$

and

$$\dot{n}_{li}(t) = \sum_{i'} \alpha_{rdi'} n_{lidi'}(t) + k_{li} n_0(t) + \sum_{j=1}^{i-1} k_{li-j} n_{lj}(t) - k n_{li}(t) - \alpha_{li} n_{li}(t) \tag{84}$$

We further give the time development for cells with more than one loci injured as

$$\begin{aligned} \dot{n}_{lidi'}(t) = {} & k_{li} n_{di'}(t) + k_{di'} n_{li}(t) + \sum_{j=1}^{i-1} k_{li-j} n_{ljdi'}(t) + \sum_{j'=1}^{i-1} k_{di'-j'} n_{lidj'}(t) \\ & - k n_{lidi'}(t) - \alpha_{li} n_{lidi'}(t) - \alpha_{di'} n_{lidi'}(t) \end{aligned} \tag{85}$$

where the cells $n_{lil'i'}(t)$ are small in number compared to $n_{lidi'}(t)$ and are neglected. The corresponding misrepair equations are

$$\dot{n}_{lid}(t) = \sum_{i'} \alpha_{mdi'} n_{lidi'}(t) + k_{li} n_d(t) + \sum_{j=1}^{i-1} k_{li-j} n_{ljd}(t) - k_s n_{lid}(t) - \alpha_{li} n_{lid}(t) \tag{86}$$

$$\dot{n}_{ldi'}(t) = \sum_{i} \alpha_{mli} n_{lidi'}(t) + k_{di'} n_l(t) + \sum_{j'=1}^{i'-1} k_{di'-j'} n_{ldj'}(t) - k_d n_{ldi'}(t) - \alpha_{di'} n_{ldi'}(t) \quad (87)$$

Note that

$$k_s = \sum_{\substack{l \epsilon s \\ i}} k_{li} \quad (88)$$

$$k_d = \sum_{\substack{l \epsilon d \\ i}} k_{li} \quad (89)$$

are the total injury rate coefficients for altered cells and cell death respectively. In the following we will treat only neoplastic transformation and clonogenic death. Other biological endpoints are easily treated in the present formalism. We will now use the repair kinetic studies of Yang et al. and the Katz formalism to evaluate the kinetic coefficients for the C3H10T1/2 system.

Katz Model for Transformations

As before in the Katz model, there are four cellular parameters to describe the response of the cells for a given biological endpoint, two of which (m, the number of targets per cell, and D_0, the characteristic x-ray dose) are extracted from the response of the cellular system to x and γ irradiation. The other two (σ_0 interpreted by Katz as the cross-sectional area of the cell nucleus within which the sensitive sites are located and κ, a measurement of the size of the sensitive site) are found principally from cell assays after track-segment irradiations with energetic, charge particles.

As discussed before the capacity of cells to accumulate sublethal damage, two modes of injury are identified: "ion-kill" (corresponding to intratrack effects) and "gamma-kill" (corresponding to intertrack effects). When the passage of a single ion damages cells, the ion-kill mode occurs. In the grain-count regime, the fraction of cells damage in the ion-kill mode is taken as $P = \sigma/\sigma_0$, where σ is the single-particle injury cross section and P is the probability of damage in the ion-kill mode. The track model assumes that a fraction of the ion dose, $(1-P)$, acts cumulatively with that from other particles to injure cells in the gamma-kill mode. The untransformed fraction of a cellular population $n_0(\infty)$, whose response parameters are m, D_0, σ_0, and κ after irradiation by a fluence of particles F, is written

$$\frac{n_0(\infty)}{n_0} = \pi_i \times \pi_\gamma \quad (90)$$

where

$$\pi_i = e^{-\sigma F} \quad (91)$$

is the ion-kill injury probability and

$$\pi_i = 1 - \left(1 - e^{-D_\gamma/D_0}\right)^m \quad (92)$$

is the gamma-kill injury probability. The gamma-kill dose fraction is

$$D_\gamma = (1-P)D \quad (93)$$

where D is the absorbed dose as in the case of cell inactivation. The single-particle injury cross section σ is given by equation (29) as in cell inactivation. The transformation yield, Y_t is written as

$$Y_t = 1 - \pi_i \times \pi_\gamma \quad (94)$$

It is the way in which transformation experiments are performed that one observes not the fraction of uninjured cells or even the transformation yield (the number of transformations per cell at risk). Rather survival experiments run concurrently and among the cell colonies

(survivors) that are observed, a fraction are transformed colonies. The fraction of surviving colonies which are transformed is called the transformation frequency, F_t. In our computational model, we find directly the transformation yield which is relatable to transformation frequency and survival fraction S as

$$Y_t = SF_t = (1 - \pi_i \times \pi_\gamma) \tag{95}$$

At low dose levels the survival fraction approaches unity so that

$$Y_t \approx F_t \tag{96}$$

To compensate, we allow for changes in the four Katz parameters as fit to frequency data. We now reconsider the relationship of the Katz model to the kinetics model.

Physics and Kinetics of Cell Injury

We again define the relationship of repair to the Katz model parameters within the context of the present repair kinetic model. We use the same approach as used in the cell survival model. We first consider the impulsive exposure of a cell population for a short time period t_r after which the cell population is given by

$$n_0(t_r) = n_0(0)e^{-kt_r} \tag{97}$$

$$n_{d1}(t_r) = k_{d1}t_r n_0(0)e^{-kt_r} \tag{98}$$

$$n_{d2}(t_r) = \left(k_{d2}t_r + \frac{1}{2!}k_{d1}^2 t_r^2\right) n_0(0)e^{-kt_r} \tag{99}$$

$$n_{d3}(t_r) = \left(k_{d3}t_r + \frac{2}{2!}k_{d2}k_{d1}t_r^2 + \frac{1}{3!}k_{d1}^3 t_r^3\right) n_0(0)e^{-kt_r} \tag{100}$$

$$n_{l1}(t_r) = k_{l1}t_r n_0(0)e^{-kt_r} \tag{101}$$

$$n_{l2}(t_r) = \left(k_{l2}t_r + \frac{1}{2!}k_{l1}^2 t_r^2\right) n_0(0)e^{-kt_r} \tag{102}$$

$$n_{l1d1}(t_r) = \frac{2}{2!}k_{l1}k_{d1}t_r^2 n_0(0)e^{-kt_r} \tag{103}$$

$$n_{l1d2}(t_r) = \left(\frac{2}{2!}k_{l1}k_{d2}t_r^2 + \frac{3}{3!}k_{d1}^2 k_{l1}t_r^3\right) n_0(0)e^{-kt_r} \tag{104}$$

$$n_{l2d1}(t_r) = \left(\frac{2}{2!}k_{d1}k_{l2}t_r^2 + \frac{3}{3!}k_{l1}^2 k_{d1}t_r^3\right) n_0(0)e^{-kt_r} \tag{105}$$

and similarly for higher order terms. After the exposure period the system is allowed to repair in the G_1 stationary phase where repair efficiencies are near maximum. The repair kinetics subsequent to exposure are described by

$$n_{lidi'}(t') = e^{-(\alpha_{li}+\alpha_{di'})t}\, n_{lidi'}(t_r) \tag{106}$$

$$n_{di}(t) = e^{-\alpha_{di}t}n_{di}(t_r) + \sum_{l'i'} \frac{\alpha_{rl'i'}}{\alpha_{l'i'}}\left[e^{-\alpha_{di}t} - e^{-(\alpha_{l'i'}+\alpha_{di})t}\right] n_{l'i'di}(t_r) \tag{107}$$

$$n_{li}(t) = e^{-\alpha_{li}t}n_{li}(t_r) + \sum_{i'} \frac{\alpha_{rdi'}}{\alpha_{di'}}\left[e^{-\alpha_{li}t} - e^{-(\alpha_{li}+\alpha_{di'})t}\right] n_{lidi'}(t_r) \tag{108}$$

$$n_{lid}(t) = \sum_{i'} \frac{\alpha_{mdi'}}{\alpha_{di'}} \left[e^{-\alpha_{li}t} - e^{-(\alpha_{li}+\alpha_{di'})t} \right] n_{lidi'}(t_r) \tag{109}$$

$$n_{ldi}(t) = \sum_{i'} \frac{\alpha_{mli'}}{\alpha_{li'}} \left[e^{-\alpha_{di}t} - e^{-(\alpha_{li'}+\alpha_{di})t} \right] n_{li'di}(t_r) \tag{110}$$

$$\begin{aligned} n_d(t) = & \sum_i \frac{\alpha_{mdi}}{\alpha_{di}} \left(1 - e^{-\alpha_{di}t}\right) n_{di}(t_r) \\ & + 2 \sum_{l'i'} \frac{\alpha_{mdi'}}{\alpha_{di'}} \frac{\alpha_{mli}}{\alpha_{li}} \left[\left(1 - e^{-\alpha_{di'}t}\right) - \left(\frac{\alpha_{di'}}{\alpha_{li} + \alpha_{di'}}\right) \left(1 - e^{-(\alpha_{li}+\alpha_{di'})t}\right) \right] n_{l'i'di}(t_r) \\ & + \sum \frac{\alpha_{mdi'}}{\alpha_{di'}} \left[\left(1 - e^{-\alpha_{li}t}\right) - \left(\frac{\alpha_{li}}{\alpha_{li} + \alpha_{di'}}\right) \left(1 - e^{-(\alpha_{li}+\alpha_{di'})t}\right) \right] n_{lidi'}(t_r) \end{aligned} \tag{111}$$

$$\begin{aligned} n_l(t) = & \sum_{i'} \frac{\alpha_{mli}}{\alpha_{li}} \left(1 - e^{-\alpha_{li}t}\right) n_{li}(t_r) \\ & + \sum_i \alpha_{mli} \sum_{i'} \frac{\alpha_{rdi'}}{\alpha_{di}} \left[\frac{1 - e^{-\alpha_{li}t}}{\alpha_{li}} - \frac{1 - e^{-(\alpha_{li}+\alpha_{di'})t}}{\alpha_{li} + \alpha_{di'}} \right] n_{lidi'}(t_r) \\ & + \sum \frac{\alpha_{mli}}{\alpha_{li}} \frac{\alpha_{rdi'}}{\alpha_{di'}} \left[1 - e^{-\alpha_{di'}t} - \left(\frac{\alpha_{di'}}{\alpha_{li} + \alpha_{di'}}\right) \left(1 - e^{-(\alpha_{li}+\alpha_{di'})t}\right) \right] n_{lidi'}(t_r) \end{aligned} \tag{112}$$

The number of uninjured cells is

$$\begin{aligned} n_0(t) = & n_0(t_r) + \sum \frac{\alpha_{rdi'}}{\alpha_{di'}} \left(1 - e^{-\alpha_{di'}t}\right) n_{di}(t_r) + \sum \frac{\alpha_{rli}}{\alpha_{li}} \left(1 - e^{-\alpha_{li}t}\right) n_{li}(t_r) \\ & + \sum \frac{\alpha_{rdi'}}{\alpha_{di'}} \frac{\alpha_{rli}}{\alpha_{li}} \left[1 - e^{-\alpha_{di'}t} - \left(\frac{\alpha_{di'}}{\alpha_{di'} + \alpha_{li}}\right) \left(1 - e^{-(\alpha_{di'}+\alpha_{li})t}\right) \right] n_{lidi'}(t_r) \\ & + \sum \frac{\alpha_{rli}}{\alpha_{li}} \frac{\alpha_{rdi'}}{\alpha_{di'}} \left[1 - e^{-\alpha_{li}t} - \left(\frac{\alpha_{li}}{\alpha_{li} + \alpha_{di'}}\right) \left(1 - e^{-(\alpha_{di'}+\alpha_{li})t}\right) \right] n_{lidi'}(t_r) \end{aligned} \tag{113}$$

and the number of survivors is

$$\begin{aligned} n_s(t) = & n_0(t_r) + \sum \left(1 - e^{-\alpha_{li}t}\right) n_{li}(t_r) + \sum \frac{\alpha_{rdi'}}{\alpha_{di'}} \left(1 - e^{-\alpha_{di'}t}\right) n_{di'}(t_r) \\ & + \sum \frac{\alpha_{rdi'}\alpha_{rli}}{\alpha_{di'}\alpha_{li}} \left[1 - e^{-\alpha_{di}t} - \left(\frac{\alpha_{di'}}{\alpha_{di'} + \alpha_{li}}\right) 1 - e^{-(\alpha_{li}+\alpha_{di'})t} \right] n_{lidi}(t_r) \\ & + \sum \frac{\alpha_{rdi'}}{\alpha_{di'}} \left[1 - e^{-\alpha_{li}t} - \left(\frac{\alpha_{li}}{\alpha_{li} + \alpha_{di'}}\right) \left(1 - e^{-(\alpha_{li}+\alpha_{di'})t}\right) \right] n_{lidi'}(t_r) \end{aligned} \tag{114}$$

If the cells are allowed to complete their repair then the number of survivors is

$$n_s(\infty) = n_0(t_r) + \sum n_{li}(t_r) + \sum \frac{\alpha_{rdi'}}{\alpha_{di'}} n_{di'}(t_r) + \sum \frac{\alpha_{rdi'}}{\alpha_{di'}} \left(\frac{\alpha_{rli} + \alpha_{di'}}{\alpha_{li} + \alpha_{di'}} \right) n_{lidi'}(t_r) \tag{115}$$

and the number of transformed cells is

$$n_l(\infty) = \sum \frac{\alpha_{mli}}{\alpha_{li}} n_{li}(t_r) + \sum \frac{\alpha_{mli}}{\alpha_{li}} \frac{\alpha_{rdi'}}{\alpha_{di'}} n_{lidi'}(t_r) \tag{116}$$

We now look to the Katz model for guidance in estimating k's. We again use the G_1 stationary phase parameters for which m_l and m_d are determined by Katz and we assume

$$\alpha_{mdi} \approx 0 \qquad i \leq m_d \tag{117}$$

$$\alpha_{mli} \approx 0 \qquad i \leq m_l \tag{118}$$

Expanding the Katz model in the low dose limit and equating to the lowest surviving terms in equations (115) and (116) results in

$$k_{dm_d} t_r = \sigma_d F \tag{119}$$

$$k_{d1} t_r = (m_d!)^{\frac{1}{m_d}} \frac{D_{\gamma_d}}{D_{0d}} \tag{120}$$

$$k_{lm_l} t_r = \sigma_l F \tag{121}$$

$$k_{l1} t_r = (m_l!)^{\frac{1}{m_l}} \frac{D_{\gamma_l}}{D_{0l}} \tag{122}$$

where $\sigma_d, m_d, D_{\gamma d}, D_{0d}$ are the usual Katz functions and parameters for cell death and $\sigma_l, m_l, D_{\gamma l}, D_{0l}$ correspond to the values for cell transformation. The α_{di} and α_{rdi} will be taken from our earlier study of cell survival and the α_{li} and α_{rli} will be found by analysis of the data of Yang et al.

The series solutions given by equations (115) and (116) converge slowly at high dose and it is convenient to perform some of the summations in closed form. For example, equation (115) may be written as

$$n_s(\infty) = n_0 e^{-k_d t_r} + \sum_{i'=1}^{m_d-1} \frac{\alpha_{rdi'}}{\alpha_{di'}} \left[n_{di'}(t_r) + \sum_{i=1}^{\infty} \left(\frac{\alpha_{rli} + \alpha_{di'}}{\alpha_{li} + \alpha_{di'}} \right) n_{lidi'}(t_r) \right] \tag{123}$$

with corresponding values for equation (116) as

$$\begin{aligned} n_l(\infty) = \left(e^{k_s t_r} - 1 \right) & \left[e^{-kt_r} n_0 + \sum_{i'=1}^{m_d-1} \frac{\alpha_{rdi'}}{\alpha_{di'}} n_{di'}(t_r) \right] \\ & - \sum_{i=1}^{m_l-1} \frac{\alpha_{rli}}{\alpha li} \left[n_{li}(t_r) + \sum_{i'=1}^{m_d-1} \frac{\alpha_{rdi'}}{\alpha_{di'}} n_{lidi'}(t_r) \right] \end{aligned} \tag{124}$$

These expressions apply to both the delayed plating experiments ($\alpha_r \approx \alpha$) as well as the immediate plating experiments of Yang et al. provided the appropriate α's are used.

Delayed Plating Studies

Yang and coworkers have utilized the following protocol, G_1 stationary cells are given a high dose rate exposure. G_1 stationary repair kinetics are utilized by retaining the population in G_1 phase for 24 hours before plating and scoring the cell modifications. Exponential phase repair kinetics are envoked by plating the cells immediately following exposure. The scoring of these protocols relate to the repair efficiency of an exponential population. Experiments with variable delay times allows evaluation of the repair rates. The delayed plating and immediate plating experiments are described by equations (115) and (116) with repair coefficients for G_1 stationary and exponential populations respectively. Description of the variable delay experiment require further development.

The cell populations subsequent to exposure are described by equations (106) to (112) where t is the time period. If at time t (delay time) the cells are plated then the final populations are given as

$$n_s(\infty) = n_0(t) + \sum n_{li}(t) + \sum \frac{\alpha'_{rd'}}{\alpha'_{di'}} n_{di'}(t) + \sum \frac{\alpha'_{rdi'}}{\alpha'_{di'}} \left(\frac{\alpha'_{rli} + \alpha'_{di}}{\alpha'_{li} + \alpha'_{di}} \right) n_{lidi}(t) \tag{125}$$

$$n_l(\infty) = n_l(t) + \sum_i \frac{\alpha'_{mli}}{\alpha'_{li}} n_{li}(t) + \sum_{ii'} \frac{\alpha'_{mli}}{\alpha'_{li}} \frac{\alpha'_{rdi'}}{\alpha'_{di'}} n_{lidi'}(t) \tag{126}$$

where the α coefficients are the G_1 stationary values and α' coefficients are the exponential phase values. The coefficients for cell death from our earlier studies are given in table 3. We have used the transformation studies of Yang et al. to determine the transformation repair coefficients using the Katz parameters in table 4a. The results for x-ray exposures are shown in figure 14. The original Katz parameters were fit to transformation frequency whereas the coefficients in our model relate to transformation yield. As a result we made some adjustments in the Katz parameters in arriving at our results in figure 14. It is difficult to ascribe the quality of fit to Yang's data due to scatter in the experiments. What is certain is that $m_l = 3$ is the only value consistent with the immediate plating data. The corresponding results are shown in figures 15 and 16 for various ions. The scattering in the transformation data limits our ability to evaluate the model.

CELL CYCLE RADIATION SURVIVAL MODEL

Living cells are found to proceed through a series of events leading to cell division referred to as the cell cycle. There are two significant events denoted by S-phase (synthesis of DNA material) and M-phase (cell division). These phases are separated by two gaps called G_1 (following mitosis) and G_2 (following S and preceding M). The cell cycle may be limited by the physical/chemical environment, interaction with adjacent cells, or available nutrients. Indeed, the growth of specialized tissues in complex organisms is controlled by cell contact interaction and exchange of growth controlling chemical compounds (Allen 1962).

The role of repair in radiobiological response was elegantly presented by Fritz-Niggli (1988). The (early) S- and M-phases appear accident prone for which G_1 and G_2 are instrumental in making repairs. Evidence of these facts lie in the following observations. First, the errors of the S- and M-phases are normally repaired, otherwise life would not exist (Fritz-Niggli,

TABLE 4a. KATZ C3H10T1/2 CELL PARAMETERS

	σ_0, cm^2	k	m	D_0, GY
Survival	5×10^{-7}	750	3	2.8
Transformation	7×10^{-11}	475	3	117

TABLE 4b. TRANSFORMATION REPAIR RATES (h^{-1}) AND REPAIR EFFICIENCY

	G_1 Phase			Exponential		
i	1	2	≥ 3	1	2	≥ 3
α_i	.25	.125	$\leq .08$	.25	.125	$\leq .08$
$\alpha_{r_i} \alpha_i^{-1}$	1.0	1.0	0.0	.99	.70	0.0

1988). Second, radiation injury sustained in (early) S- and M-phases is more likely to end the cell line than injury received in the (early) G_1- and G_2-phase (especially early G_1 and late G_2, Sinclair, 1968). The cell cycle progression can be blocked (delayed) in G_1 or G_2 by injury sustained in that phase until the injury is repaired (Mitchison, 1971)). These simple facts alone provide insight as to the biological response of more complex organisms.

A tissue from a complex organism exhibits a distribution of cells over various phases. The highly differentiated tissues are predominantly stationary G_1 and are well known to be radiation resistant. That (stationary) G_1 repair systems are highly efficient would seem necessary to preserve complex organisms. Stem cell tissues have significant populations of M- and especially S-phase cells and are in part responsible for acute radiation syndrome in higher animals. Immature individuals are more sensitive than adults and the embryo is most sensitive of all. Clearly, a viable model of radiation response must account for the varying repair kinetics for the differing cell phases and the distribution of tissue cells within the cell cycle.

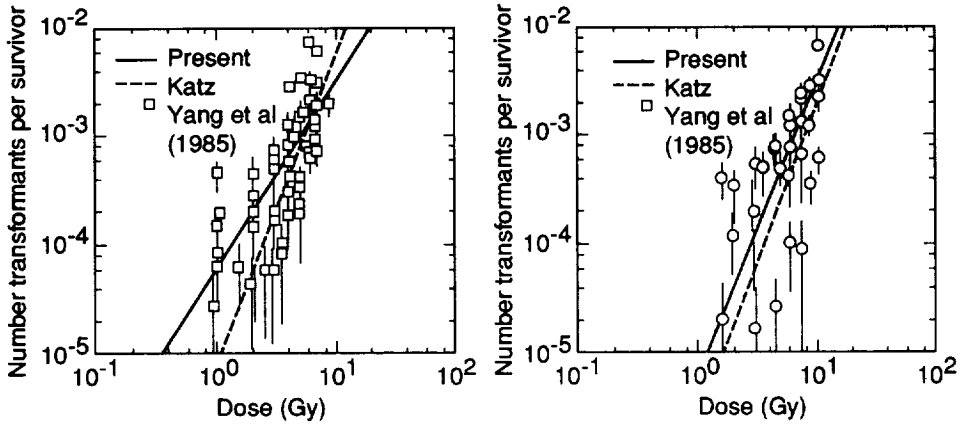

(a) Immediate plating x-ray. (b) Delayed plating x-ray.

Figure 14. Transformation frequencies for x-ray exposures.

Ultimately, the radiation response of an organism or tissue is determined by the biological processes of individual cells. It is the specific molecular structures and their physical interaction with passing ionizing radiation which initiates the response mechanisms, but the cell's ability to repair such physical insult is a primary determinant of cell sensitivity to ionizing radiation. In that the progression of cell chemistry is controlled by cellular environmental factors, individual cell response is governed in part by external factors for which there is some experimental control. Indeed, the environmental factors existing within tissue systems are ultimately related to carcinogenic response. From this viewpoint, cell repair kinetics and the relation to cell environment is of fundamental importance in understanding radiation effects in biological systems.

In the present section, we show how to develop a more comprehensive model of the cell kinetics. The present model lacks age dependence within the cycle. We still rely on the Katz model for a description of the physics of the track structure. The cell kinetics are represented by an unbounded set of coupled linear differential equations describing multiples of lesions within the cell. The kinetic coefficients in the model are to be determined from repair dependent cell response data.

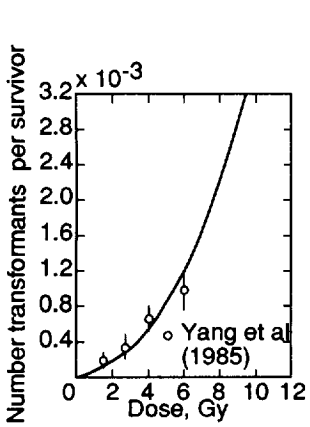

(a) Delayed plating Ne^{20} (425 MeV/n).

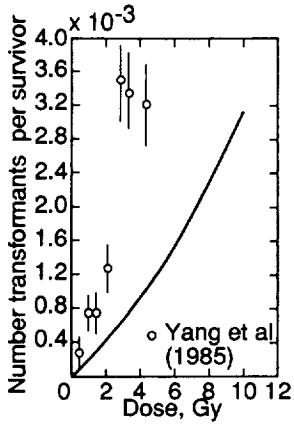

(b) Delayed plating Si^{28} (320 MeV/n).

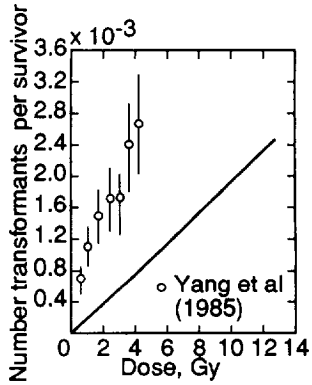

(c) Delayed plating Si^{28} (670 MeV/n).

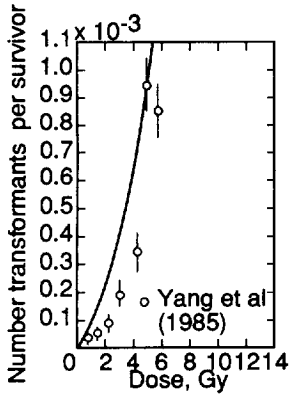

(d) Delayed plating Ar^{40} (330 MeV/n).

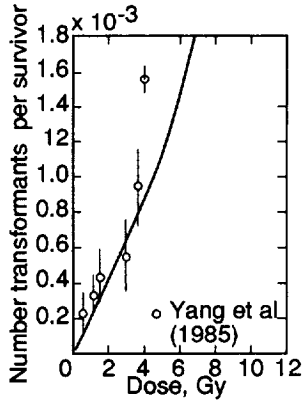

(e) Delayed plating Fe^{56} (600 MeV/n).

Figure 15. Transformation frequencies for various ions. Delayed plating.

Cell Cycle Kinetics

Cell cultures of higher animal cells cycle in approximately 24 hours. The cell populations n_1, n_2, n_3, n_4 represent the phases G_1, S, G_2, M and satisfy the approximate equations

$$\dot{n}_1 = 2n_4/\tau_4 - n_1/\tau_1 \tag{127}$$

$$\dot{n}_2 = n_1/\tau_1 - n_2/\tau_2 \tag{128}$$

$$\dot{n}_3 = n_2/\tau_2 - n_3/\tau_3 \tag{129}$$

$$\dot{n}_4 = n_3/\tau_3 - n_4/\tau_4 \tag{130}$$

The time spent in mitosis, τ_4, is quite small compared to the other phases so that n_4 is in near equilibrium with n_3 so that the approximate equations can be used

$$\dot{n}_1 = 2n_3/\tau_3 - n_1/\tau_1 \tag{131}$$

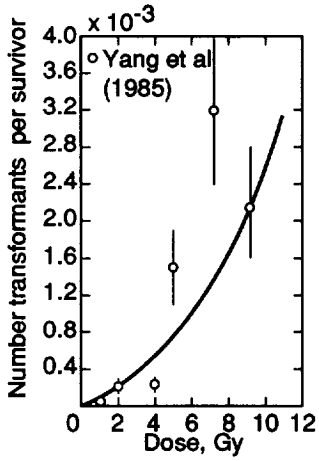

(a) Immediate plating C^{12} (474 MeV/n).

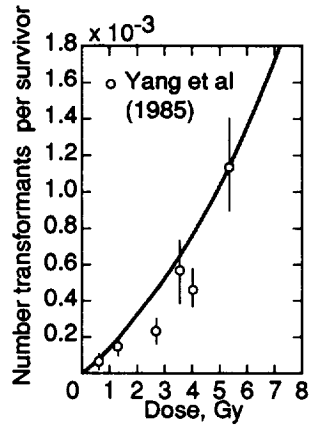

(b) Immediate plating Ne^{20} (425 MeV/n).

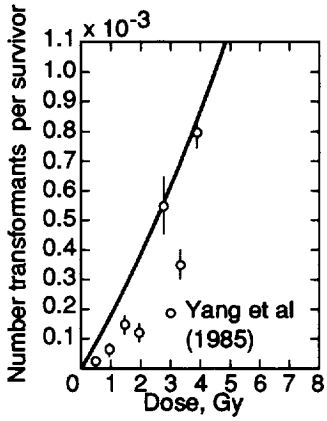

(c) Immediate plating Si^{28} (670 MeV/n).

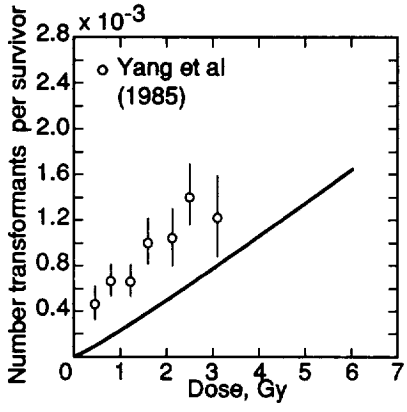

(d) Immediate plating Si^{28} (320 MeV/n).

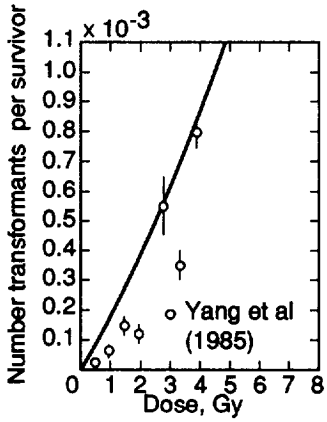

(e) Immediate plating Ar^{40} (330 MeV/n).

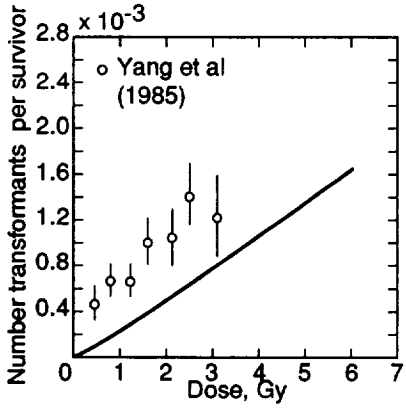

(f) Immediate plating Fe^{56} (300 MeV/n).

Figure 16. Transformation frequencies for various ions. Immediate plating.

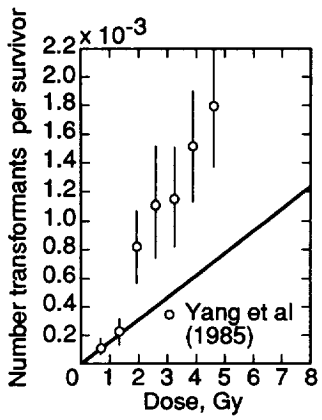

(g) Immediate plating Fe^{56} (400 MeV/n).

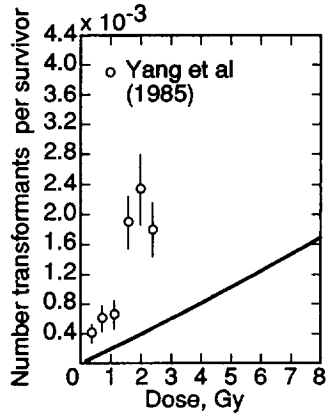

(h) Immediate plating Fe^{56} (600 MeV/n).

Figure 16. Concluded.

$$\dot{n}_2 = n_1/\tau_1 - n_2/\tau_2 \tag{132}$$

$$\dot{n}_3 = n_2/\tau_2 - n_3/\tau_3 \tag{133}$$

Furthermore, these three phases are sometimes of near equal duration so that $\tau = \tau_1 \approx \tau_2 \approx \tau_3$. One may then show that for an initial G_1 population that

$$n_1 = n_0\, e^{-t/\tau} + n_0\, \frac{1}{3}\left(\frac{t}{\tau}\right)^3 e^{-t/\tau} + n_0\, \frac{2}{3\cdot 4\cdot 5\cdot 6}\left(\frac{t}{\tau}\right)^6 e^{-t/\tau} + \ldots \tag{134}$$

$$n_2 = n_0\, \frac{t}{\tau}\, e^{-t/\tau} + n_0\, \frac{1}{3\cdot 4}\left(\frac{t}{\tau}\right)^4 e^{-t/\tau} + \ldots \tag{135}$$

$$n_3 = n_0\, \frac{1}{2}\left(\frac{t}{\tau}\right)^2 e^{-t/\tau} + n_0\, \frac{1}{3\cdot 4\cdot 5}\left(\frac{t}{\tau}\right)^5 e^{-t/\tau} + \ldots \tag{136}$$

The total cell population is given by

$$n_{\text{tot}} = n_0 + n_0 \sum_j \frac{(2^j - 1)}{(3j)!}\left(\frac{t}{\tau}\right)^{3j} e^{-t/\tau} + n_0 \sum_j \frac{(2^j - 1)}{(3j+1)!}\left(\frac{t}{\tau}\right)^{3j+1} e^{-t/\tau} + n_0 \sum_j \frac{(2^j - 1)}{(3j+2)!}\left(\frac{t}{\tau}\right)^{3j+2} e^{-t/\tau} \tag{137}$$

We note that the present cell phase model is never fully synchronized resulting from the lack of an age variable within each phase. This is not a serious limitation since real cells loose their synchronization after about two cycles. More importantly, cell repair efficiency varies within a given phase which must be treated in a comprehensive model. Equations (130) to (136) will be used herein to describe the cell phase kinetics for exponential populations. The time development of an exponential population is shown in figure 17. The first generation phase populations are shown separately as is the second generation G_1 population. Growth limited populations require $\tau_1 \gg \tau_2 + \tau_3$ and a corresponding generalization of equation (137).

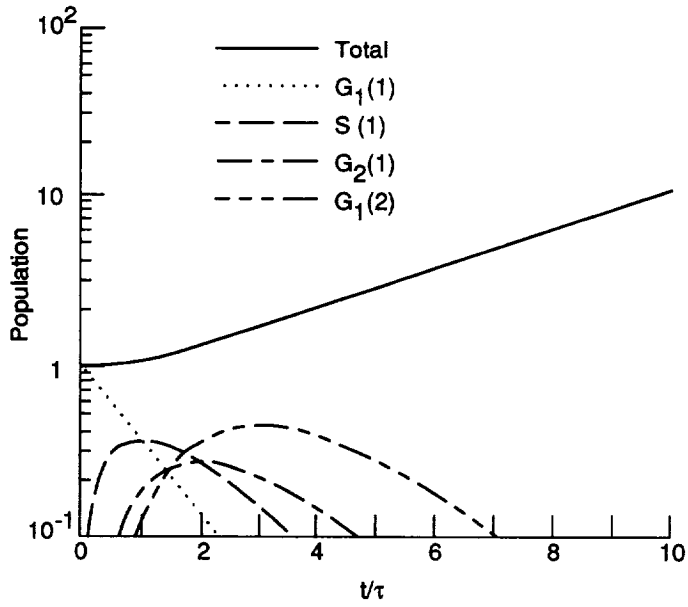

Figure 17. Population distribution for cell cycle model.

Tissue systems are noted for their low degree of mitotic activity obtained in the above model for $\tau_1 \gg \tau_2 \simeq \tau_3 = \tau$. This leaves the n_2 and n_3 populations in near equilibrium with the n_1 population as

$$n_2 \simeq \tau_2 n_1/\tau_1 \tag{138}$$

$$n_3 \simeq \tau_3 n_1/\tau_1 \tag{139}$$

and the solution to equation (131) is

$$n_1(t) \simeq n_1(0)\, e^{t/\tau_1} \tag{140}$$

At any given time S-, G_2- and M-phase cells will be very few as a result of $\tau/\tau_1 \ll 1$. If τ_2, τ_3 are the same as for the exponential population above the doubling time for n_1 given by equation (140) is on the order of one year. We now consider the coupling of the cell phase kinetics with the cell repair kinetics as we have used before.

RADIATION INJURY AND REPAIR

We define $n_{si}(t)$ as the number of cells in phase labeled by s which have received a number i of radiation-induced lesions at any time, t, in the original population of cells, n_{so} $(t = 0)$. Lacking a mechanistic foundation, we will consider an average lesion and neglect differences in the types that will occur. More important will be an accounting of the number of lesions that do occur. We also assume herein that cell death is independent of where the lesions occur; the treatment of other biological endpoints will require the differentiation among specific loci within the DNA and was dealt with in the previous sections.

We assume that these lesions are subsequently chemically stabilized and may either restore the cell to its initial structure or leave permanent changes which alter the cell function. The kinetics of cellular repair will, to a large degree, determine the time development of the initial population of radiation-produced lesions. Survival curves are based on measurements long after the induction of lesions by radiation and are functions of both the track structure of the radiations and the repair kinetics. The progression in time of the cellular populations

$n_{si}(t)$ is assumed to be governed by a coupled set of linear first-order differential equations reflecting the losses and gains by radiation injury and repair. The rate at which radiation-induced lesions are produced is denoted k_i and is assumed to be cell phase independent. The k_i scale linearly with the flux of ionizing radiations and will depend on particle type, i.e., track structure. The mean lesion repair rate (averaged over loci with i-fold lesions) is denoted α_{si} and the number of i-fold lesions repaired per unit time is then $\alpha_{si}\ n_{si}$. The equations within a given cell phase which determine the change in the lesion populations with time are given by

$$\dot{n}_{so} = \sum_{i=1}^{\infty} \alpha_{sr_i}\ n_{si} - k\ n_{so} \tag{141}$$

$$\dot{n}_{si} = \sum_{j=0}^{i-1} k_{i-j}\ n_{sj} - k\ n_{si} - \alpha_{si}\ n_{si} \tag{142}$$

where the subscript i of n_{si} denotes the multiplicity of (chemical) lesions. We allow for lesion misrepair in the model by the time evolution equation for misrepaired cell m as

$$\dot{m}_s = \sum_{i=1}^{\infty} \alpha_{smi}\ n_{si} \tag{143}$$

Conservation of cell number dictates $\alpha_{si} = \alpha_{sri} + \alpha_{smi}$ and $k = k_1 + k_2 + \ldots$ within a given cell phase. In equations (140) and (141), we have assumed the rates k_i are independent of possible previous lesions; however, this restriction could be lifted if necessary. The lesions are chemically active species neutralized by enzyme activity and radical recombination at rate constants α_{si}. The α_{sri} and α_{smi} are repair and misrepair rates for the lesion to be restored (α_{sr}) or permanently injured (α_{sm}). This is not the most general model but reasonably represents the essential kinetics for cell survival.

The effects of radiation injury on the cell cycle kinetics has been reviewed by Casarett (1968) and the implications will now be modeled. Cell populations with no lesions (including those which are repaired) undergo the usual cell cycle. We assume injured cells progress to G_2 where repairs are completed (G_2 block) before mitosis. The appropriate equations are given as

$$\dot{n}_{10} = 2\ n_{30}/\tau_3 - n_{10}/\tau_1 - k\ n_{10} + \sum_{i=1} \alpha_{1ri}\ n_{1i} \tag{144}$$

$$\dot{n}_{1i} = -\beta_i\ n_{1i}/\tau_1 + \sum_{j=0}^{i-1} k_{i-j}\ n_{1j} - k n_{1i} - \alpha_{1i}\ n_{1i} \tag{145}$$

$$\dot{n}_{20} = n_{10}/\tau_1 - n_{20}/\tau_2 - k\ n_{20} + \sum_{i=1} \alpha_{2ri}\ n_{2i} \tag{146}$$

$$\dot{n}_{2i} = \beta_i\ n_{1i}/\tau_1 - \gamma_i n_{2i}/\tau_2 + \sum_{j=0}^{i-1} k_{i-j}\ n_{2j} - k\ n_{2i} - \alpha_{2i}\ n_{2i} \tag{147}$$

$$\dot{n}_{30} = n_{20}/\tau_2 - n_{30}/\tau_3 - k\ n_{30} + \sum_{i=1} \alpha_{3ri}\ n_{3i} \tag{148}$$

$$\dot{n}_{3i} = \gamma_i n_{2i}/\tau_2 + \sum_{j=0}^{i-1} k_{i-j}\ n_{3j} - k\ n_{3i} - \alpha_{3i}\ n_{3i} \tag{149}$$

$$\dot{m}_s = \sum_{i=1} \alpha_{smi}\, n_{si} \tag{150}$$

where m_s are the number of misrepairs in a given cell phase S and are assumed to terminate the cell. The total number of cell deaths is $m = m_1 + m_2 + m_3$. In practice there is a G_1 block with a repair efficiency different from the G_1 stationary phase. This must be dealt with using a G_1 age dependent repair rate beyond the scope of the present work.

In the above equations are many parameters which must be determined. The τ_s parameters related to cell cycle times are characteristic of the cells and their environment. We will assume τ_2 and τ_3 are fixed by cell properties but τ_1 is easily affected by environmental factors. The k_i relate to the formation rates of nascent lesions and are linear in particle flux. The k_i are functions of track structure. The α's are functions of the cell repair chemistry and determine how the nascent lesions are ultimately resolved by the cell. In previous work we have determined the k coefficients using the Katz parameters and assumptions concerning the G_1 repair efficiencies. We will show how these methods apply to the present formalism.

Physics and Kinetics of Cell Injury

In the Katz model, it is assumed that electromagnetic radiations form single lesions with an efficiency related to D_o and generally more than one lesion ($m \geq 2$) is required to express the biological effect (cell death in the present study). It will be useful to first consider the case of irradiation in stationary G_1-phase where misrepair effects are small. If the cells are irradiated in G_1 and are held ($\tau_1 \to \infty$, τ_2, $\tau_3 \ll \tau_1$) in this phase until repair is complete, then the surviving population is from equations (143) and (144) as

$$n_{10}(\infty) = n_{10}(t_r) + \sum_{i=1}^{m-1} \left(\frac{\alpha_{1ri}}{\alpha_{1i}}\right) n_{1i}(t_r) \tag{151}$$

where assuming maximum repair in G_1 implies $\frac{\alpha_{ri}}{\alpha_i} \approx 1$ for $i < m$. Equation (151) allows us to relate the k_i coefficients to the corresponding Katz parameters as applied to the appropriate experimental protocol (namely, G_1 exposure followed by complete G_1 repair). In the kinetic model, $n_{10}(0)$ is the initial number of G_1 cells, and equation (151) is rewritten assuming maximum repair efficiency as

$$\frac{n_{10}(\infty)}{n_{10}(0)} = e^{-kt_r} + \sum_{i=1}^{m-1} k_i\, t_r\, e^{-kt_r} + \frac{1}{2!}\, k_1\, t_r \sum_{i=1}^{m-1} k_i\, t_r\, e^{-kt_r}$$
$$+ \frac{1}{3!}\,(k_1\, t_r)^2 \sum_{i=1}^{m-2} k_1\, t_r\, e^{-kt_r} + \ldots \tag{152}$$

We consider first the example of an $m = 3$ system. According to the Katz model, an $m = 3$ system has a γ-ray response given by

$$\frac{n_{10}(\infty)}{n_{10}(0)} \cong 1 - \left(1 - e^{-D_\gamma/D_o}\right)^3 \cong 1 - \left(\frac{D_\gamma}{D_o}\right)^3 \tag{153}$$

For γ-rays, only single-step transitions are allowed. This assumption leads to the identification applied to equation (152) if

$$k_1\, t_r \cong 6^{\frac{1}{3}} D_\gamma/D_o \tag{154}$$

$$k_m\, t_r \approx 0 \quad (m > 1) \tag{155}$$

as is appropriate for γ-rays as was assumed for inactivation in equations (41) and (42). For ions, m-step transitions may occur through multiple δ-ray production leading to a

non-zero k_m. The correspondence between the k_m and the cross section σ is then determined from the remaining Katz terms by noting for strictly ion kill kinetics

$$k_3\ t_r \cong \sigma F \tag{156}$$

$$k_2\ t_r \cong 0 \tag{157}$$

Requiring k_2 to be zero results from our matching of equation (151) and equation (34) at low dose. There may be non-zero values of k_2, but they cannot be strictly determined from the present form of Katz's theory. Radiation rates k_n for $i \gg m$ are also not considered in the Katz model. Although the k_i's may reflect both physical and chemical processes because of their empirical nature, we assume here that they are most clearly identified with the physical processes discussed by Katz. We now examine means by which repair rates can be estimated at least for some experimental cell systems.

Impulsive Exposures

The typical exposure protocol uses an intense particle beam in which exposure times are short compared to the cell cycle period and the cell repair times. The distribution of nascent lesions are then given for each phase of the cell cycle as

$$n_{s0}(t_r) = n_{s0}(0)\ e^{-kt_r} \tag{158}$$

$$n_{s1}(t_r) = n_{s0}(0)\ k_1\ t_r\ e^{-kt_r} \tag{159}$$

$$n_{s2}(t_r) = n_{s0}(0)\left[\frac{1}{2!}\ k_1^2\ t_r^2\ e^{-kt_r} + k_2\ t_r\ e^{-kt_r}\right] \tag{160}$$

$$n_{s3}(t_r) = n_{s0}(0)\left[\frac{1}{3!}\ k_1^3\ t_r^3\ e^{-kt_r} + k_1\ k_2\ t_r^2\ e^{-kt_r} + k_3\ t_r\ e^{-kt_r}\right] \tag{161}$$

and similarly for higher order terms. Equations (158) to (161) may be taken as the initial populations for the cell system described by equations (141) to (150) with the corresponding k_i coefficients taken as zero. A general solution is found as follows.

We assume a solution of the form ($i > 0$)

$$n_{si}(t) = \sum_{j=0}\left[a_{sij}\ t^j\ e^{-\nu_{1i}t} + b_{sij}\ t^j\ e^{-\nu_{2j}t} + c_{sij}\ t^j\ e^{-\nu_{3j}t}\right] \tag{162}$$

The initial conditions are met as

$$a_{1i0} = n_{1i}(0) \tag{163}$$

$$b_{2i0} = n_{2i}(0) \tag{164}$$

$$c_{3i0} = n_{3i}(0) \tag{165}$$

with all other a_{sio}, b_{sio}, c_{sio} being zero and

$$\nu_{1i} = \beta_i\ \tau_1^{-1} + \alpha_{1i} \tag{166}$$

$$\nu_{2i} = \gamma_i\ \tau_2^{-1} + \alpha_{2i} \tag{167}$$

$$\nu_{3i} = \alpha_{3i} \tag{168}$$

The remaining coefficients of equation (162) are found to satisfy recurrence relations which allows evaluation of the sums term-by-term. The recurrence relations for each cell phase are distinct with the following valid for G_1-phase ($s = 1$)

$$(j+1)a_{1ij+1} = 0 \tag{169}$$

$$(j+1)b_{1ij+1} = (\nu_{2i} - \nu_{1i})\, b_{1ij} + \gamma_i\, b_{2ij}/\tau_2 \tag{170}$$

$$(j+1)c_{1ij+1} = (\nu_{3i} - \nu_{1i})\, c_{1ij} + \gamma_i\, c_{2ij}/\tau_2 \tag{171}$$

The corresponding S-phase relations ($s = 2$) are

$$(j+1)a_{2ij+1} = (\nu_{1i} - \nu_{2i})\, a_{2ij} + \beta_i\, a_{1ij}/\tau_1 \tag{172}$$

$$(j+1)b_{2ij+1} = \beta_i\, b_{1ij}/\tau_1 \tag{173}$$

$$(j+1)c_{2ij+1} = (\nu_{3i} - \nu_{2i})\, c_{2ij} + \beta_i\, c_{1ij}/\tau_1 \tag{174}$$

with similar G_2-phase relations ($s = 3$)

$$(j+1)a_{3ij+1} = (\nu_{1i} - \nu_{3i})\, a_{3ij} + \gamma_i\, a_{2ij}/\tau_2 \tag{175}$$

$$(j+1)b_{3ij+1} = (\nu_{2i} - \nu_{3i})\, b_{3ij} + \gamma_i\, b_{2ij}/\tau_2 \tag{176}$$

$$(j+1)c_{3ij+1} = \gamma_i\, c_{2ij}/\tau_2 \tag{177}$$

In writing the solution in the form of equation (162) we have found the repair solutions to run in three separate cycles according to the initial population distributions prior to exposure. Clearly a G_1 stationary population cycles through the 'a' coefficients only with the b's and c's all identically zero. Similarly, a synchronized S-phase exposed population cycles according to the 'b' coefficient recurrence relations while the 'c' coefficients are exclusively related to exposure in G_2-phase. Clearly an exponential population excites all three recurrence relations according to the equilibrium distribution of the cell population.

First Generation Kinetics

According to our general kinetic equations (141) to (150), injured cells are blocked in G_2 until repairs are complete. The repair kinetics in the first generation of injured cells determine the fate of the cell. This is not in complete accordance with experimental observation in which one or two cell divisions are relatively common before the cell line is terminated. The recurrence relations among the a, b, and c coefficients may be solved in closed form to generate the cycle dependent repair processes.

a. G_1 repair cycle. We first consider the repair cycle of G_1-phase injured cells using recurrence relations given by equations (169), (172) and (175). The G_1 repair cycle is found to be given by

$$n_{1i}(t) = n_{1i}(0)\, e^{-\nu_{1i}t} \tag{178}$$

$$n_{2i}(t) = n_{1i}(0)\, \frac{\beta_i}{\tau_1} \left[\frac{e^{-\nu_{2i}t} - e^{-\nu_{1i}t}}{\nu_{1i} - \nu_{2i}} \right] \tag{179}$$

$$n_{3i}(t) = n_{1i}(0)\, \frac{\beta_i}{\tau_1}\, \frac{\gamma_i}{\tau_2}\, e^{-\nu_{1i}t} \sum_{j=2}^{\infty} \frac{t^j}{j!} \sum_{\ell=0}^{j} (\nu_{1i} - \nu_{2i})^{\ell} (\nu_{1i} - \nu_{3i})^{j-\ell} \tag{180}$$

$$m_1(t) = \sum_{i>0} n_{1i}(0)\, \frac{\alpha_{m1i}}{\nu_{1i}} \left(1 - e^{-\nu_{1i}t}\right) \tag{181}$$

$$m_2(t) = \sum_{i>0} n_{1i}(0)\ \frac{\beta_i}{\tau_1}\frac{\alpha_{m2i}}{(\nu_{1i}-\nu_{2i})}\left[\frac{1}{\nu_{2i}}\left(1-e^{-\nu_{2i}t}\right)-\frac{1}{\nu_{1i}}\left(1-e^{-\nu_{1i}t}\right)\right] \tag{182}$$

$$m_3(t) = \sum_{i>0} n_{1i}(0)\ \frac{\beta_i}{\tau_1}\frac{\gamma_i}{\tau_2}\frac{\alpha_{m3i}}{\nu_{1i}}\sum_{j=2}^{\infty}\left[1-\frac{\Gamma(j+1,\nu_{1i}t)}{j!}\right]\sum_{\ell=0}^{j}\frac{(\nu_{1i}-\nu_{2i})^{\ell}\ (\nu_{1i}-\nu_{2i})^{j-\ell}}{\nu_{1i}^{j}} \tag{183}$$

The above are solutions for cycling cell systems and approach the stationary G_1 repair kinetics for $\tau_1 \to \infty$ with τ_2 and τ_3 finite. Such a limit corresponds to the delayed plating experiments of Yang et al. (1989). The stationary phase solutions are given as

$$n_{1i}(t) = n_{1i}(0)\ e^{-\alpha_{1i}t} \tag{184}$$

$$m_1(t) = \sum_{i>0} n_{1i}(0)\ \frac{\alpha_{m1i}}{\alpha_{1i}}\left(1-e^{-\alpha_{1i}t}\right) \tag{185}$$

with $n_{2i}(t)$, $n_{3i}(t)$, $m_2(t)$, and $m_3(t)$ all zero. If complete repair is allowed in G_1-phase as in Yang et al. (1989) delayed plating experiments then the misrepaired population is

$$m(\infty) = \sum_{i>0} n_{1i}(0)\ \frac{\alpha_{m1i}}{\alpha_{1i}} \tag{186}$$

as we found earlier (Wilson and Cucinotta, 1991). The misrepair ratios were found near zero for $m < 3$ as required for the sigmoid shape in the x-ray survival data and recovery of the Katz model at low dose.

Herein we assume G_1 and G_2 misrepair is near zero so that the cycling G_1 exposures have total misrepair given by

$$m(\infty) \simeq \sum_{i>1} n_{1i}(0)\ \frac{\beta_i}{\tau_1}\ \frac{\alpha_{m2i}}{\nu_{1i}\nu_{2i}} \tag{187}$$

which should match our earlier results for the immediately plated exposures as

$$\frac{\beta_1}{\tau_1}\ \frac{\alpha_{m21}}{\nu_{11}\nu_{21}} = 0.3 \tag{188}$$

$$\frac{\beta_2}{\tau_1}\ \frac{\alpha_{m22}}{\nu_{12}\nu_{22}} = 0.88 \tag{189}$$

We have no means for evaluating the β_i and γ_i at this time and so we assume the cell cycle times of injured cells are the same as the unexposed population (i.e., $\beta_i = \gamma_i = 1$). The corresponding misrepair coefficients are then found to be

$$\alpha_{m21} = 0.3\tau_2^{-1}\,(1+\alpha_{11}\ \tau_1)\,(1+\alpha_{21}\ \tau_2) \tag{190}$$

$$\alpha_{m22} = 0.88\tau_2^{-1}\,(1+\alpha_{12}\ \tau_1)\,(1+\alpha_{22}\ \tau_2) \tag{191}$$

where the τ_1 and τ_2 are those associated with the Yang et al. experiments ($\tau_1 \simeq 4$ hr and $\tau_2 \simeq 10$ hr resulting in $\alpha_{m21}/\alpha_{21} \simeq 0.84$ and $\alpha_{m22}/\alpha_{22} \simeq 1$).

b. S-repair cycle. Cells injured in the S-phase cycle are described through the b coefficient recurrence relations as given by equations (170), (173), and (176). The solutions for the S-repair cycle is given as

$$n_{1i}(t) = 0 \tag{192}$$

$$n_{2i}(t) = n_{2i}(0)\ e^{-\nu_{2i}t} \tag{193}$$

$$n_{3i}(t) = n_{2i}(0)\ \frac{\gamma_i}{\tau_2}\left[\frac{e^{-\nu_{3i}t}\ -e^{-\nu_{2i}t}}{\nu_{2i}-\nu_{3i}}\right] \tag{194}$$

$$m_1(t) = 0 \tag{195}$$

$$m_2(t) = \sum_{i>0} \frac{\alpha_{m2i}}{\nu_{2i}}\, n_{2i}(0)\, \left(1 - e^{-\nu_{2i}t}\right) \tag{196}$$

$$m_3(t) = \sum_{i>0} \frac{\alpha_{m3i}}{(\nu_{2i} - \nu_{3i})}\, \frac{\gamma_i}{\tau_2}\, n_{2i}(0) \left[\frac{1}{\nu_{3i}}\left(1 - e^{-\nu_{3i}t}\right) - \frac{1}{\nu_{2i}}\left(1 - e^{-\nu_{2i}t}\right)\right] \tag{197}$$

The total number of misrepaired cells following a single impulsive exposure is

$$m(\infty) = \sum_{i>0} \left[\frac{\alpha_{m2i}}{\nu_{2i}} + \frac{\alpha_{m3i}}{\nu_{2i}\nu_{3i}}\, \frac{\gamma_i}{\tau_2}\right] n_{2i}(0) \tag{198}$$

Since in our current understanding $\tau_1 \nu_{1i} \beta_i^{-1} > 1$ we see that the misrepair rate of the S-phase injury is higher than the G_1-phase injury cycle. This is not surprising since repair during the G_1-phase is very efficient.

c. G_2-repair cycle. The G_2-repair cycle is simplified by the complete G_2 block assumed in the present model. The c coefficient recurrence relations (171), (174), and (177) give solutions

$$n_{1i}(t) = n_{2i}(t) = 0 \tag{199}$$

$$n_{3i}(t) = n_{3i}(0)\, e^{-\nu_{3i}t} \tag{200}$$

$$m_1(t) = m_2(t) = 0 \tag{201}$$

$$m_3(t) = \sum_{i>0} \frac{\alpha_{m3i}}{\nu_{3i}}\, n_{3i}(0) \left(1 - e^{-\nu_{3i}t}\right) \tag{202}$$

The total misrepair fraction is near zero since the G_2-phase repair efficiency is assumed near unity and shows similar survival characteristics as the stationary G_1-phase repair kinetics.

d. Exponential population repair kinetics. Exposure of an exponential population is described as a superposition of the previous solutions. The initial irradiated cell population is the equilibrium distribution in which

$$n_s(0) = \frac{\tau_s}{\sum_{s'} \tau_{s'}}\, n_0(0) \tag{203}$$

where $n_0(0)$ is the total cell population. The initial distribution of injured cells are given by equations (158) to (161). Subsequent to exposure, the misrepair is described by equations (178) to (202) and the total misrepair population is given as

$$\begin{aligned} m(\infty) &\approx \sum_{i>0} \frac{1}{\tau_1}\, \frac{\alpha_{m2i}}{\nu_{1i}\nu_{2i}}\, n_{1i}(0) + \sum_{i>0} \frac{\alpha_{m2i}}{\nu_{2i}}\, n_{2i}(0) \\ &= \sum_{i>0} \left(\frac{1}{\tau_c \nu_{1i}} + \frac{\tau_2}{\tau_c}\right) \frac{\alpha_{2mi}}{\nu_{2i}}\, n_i(0) \end{aligned} \tag{204}$$

where

$$\tau_c = \sum_s \tau_s \tag{205}$$

$$n_i(0) = \sum_s n_{si}(0) \tag{206}$$

e. Tissue systems repair kinetics. The main characteristic of tissue systems represented in the present model is the excessive time spent in the G_1-phase. The cell distribution is then approximately

$$n_1 = \frac{\tau_1}{\tau_c}\, n_0 \simeq n_0 \tag{207}$$

$$n_2 = \frac{\tau_2}{\tau_c}\, n_0 \simeq \frac{\tau_2}{\tau_1}\, n_0 \tag{208}$$

$$n_3 = \frac{\tau_3}{\tau_c}\, n_0 \simeq \frac{\tau_3}{\tau_1}\, n_0 \tag{209}$$

Repair within the G_1 population after exposure is given by equations (184) and (185) so that

$$m_1(\infty) = \sum_{i>0} \frac{\alpha_{m1i}}{\alpha_{1i}}\, n_{1i}(0) \tag{210}$$

The repair for S-phase exposures are

$$m_2(\infty) = \sum_{i>0} \frac{\alpha_{m2i}}{\nu_{2i}}\, n_{2i}(0) \tag{211}$$

$$m_3(\infty) = \sum_{i>0} \frac{1}{\tau_2}\, \frac{\alpha_{m3i}}{\nu_{2i}\nu_{1i}} n_{2i}(0) \tag{212}$$

while G_2 injury results in

$$m_3(\infty) = \sum_{i>0} \frac{\alpha_{m3i}}{\nu_{3i}}\, n_{3i}(0) \tag{213}$$

Due to the assumed efficient repair in G_2 we see that $m_3(\infty)$ given by equations (212) and (213) are inferior to $m_2(\infty)$ of equation (211). The total misrepair is then

$$m(\infty) = \sum_{i>0} \left[\frac{\alpha_{m1i}}{\alpha_{1i}} + \frac{\tau_2}{\tau_1}\, \frac{\alpha_{m2i}}{\nu_{2i}} \right] n_{2i}(0) \tag{214}$$

In the event that $\frac{\tau_2}{\tau_1} \ll \frac{\alpha_{m1i}}{\alpha_{1i}}$ then the population response is similar to G_1-phase stationary populations as is usually the case.

Discussion

With the formalism of cell injury and repair within the cell cycle presented in this last section there is some hope of deriving a more complete description of the cell kinetic problem. However, a more complete model must first treat the age dependence within the phase. For example, the G_1 phase must be treated as an early G_1 and late G_1 as a minimum requirement. This we know since the G_1 block repair efficiency is similar to the S-phase repair efficiency and not the G_1 stationary repair efficiency. With such a complete model one may turn to the issue of cell progression within a tissue system. Such issues are critical for understanding biological response.

REFERENCES

Allen, J. M.; 1962: *The Molecular Control of Cellular Activity.* McGraw-Hill, Inc. New York.

Bettega, D.; Calzolari, P.; Ottolenghi A.; and Tallone Lombardi, L.; 1990: Oncogenic Transformation Induced by High and Low LET Radiations. *Radiat. Prot. Dosim.* vol. 31, pp. 279–283.

BEIR V; 1990: *Health Effects of Exposure to Low Levels of Ionizing Radiation*, Washington, D.C.; National Academy Press.

Casarett, A. P.; 1968: *Radiation Biology*, Prentice-Hall, Englewood Cliffs, NJ.

Cartwright, D. C.; Trajmar, S.; Chutjian, A.; and Williams, W.; 1977: Electron Impact Excitation of the Electronic States of N_2. II. Integral Cross Sections at Incident Energies From 10 to 50 eV. *Phys. Review A*, vol. 16, no. 3, pp. 1041–1051.

Charlesby, A.; 1967: Radiation Mechanisms in Polymers, In *Irradiation of Polymers*, R. F. Gould, ed., American Chemical Society, Washington, D.C., pp. 1–21.

Crawford-Brown, D. J.; and Hoffmann, W.; 1990: A Generalized State-vector Model for Radiation-induced Cellular Transformation. *Int. J. Radiat. Biol.*, vol. 57, pp. 407–423.

Cucinotta, F. A.; Katz, R.; Wilson, J. W.; Townsend, L. W.; Nealy J. E.; and Shinn, J. L.; 1991a: *Cellular Track Model of Biological Damage to Mammalian Cell Cultures From Galactic Cosmic Rays.* NASA TP-3055.

Cucinotta, F. A.; Katz, R.; Wilson, J. W.; Townsend, L. W.; Shinn, J. L.; and Hajnal, F.; 1991b: Biological Effectiveness of High Energy Protons: Target Fragmentation. *Radiat. Res.*, vol. 127, pp. 130–137.

Curtis, S. B.; 1986: Lethal and Potentially Lethal Lesions Induced by Radiation—A Unified Repair Model. *Radiat. Res.*, vol. 106, pp. 252–270.

Fritz-Niggli, H.; 1988: The Role of Repair Processes in Cellular and Genetic Response to Radiation. In: *Terrestrial Space Radiation and It's Biological Effects*, Edited by P. D. McCormack, C. E. Swenberg and H. Bücker, Plenum Press, New York.

Frost, A. A.; and Pearson, R. G.; 1962: *Kinetics and Mechanisms.* John Wiley and Sons, NY.

Goodhead, D. T.; 1985: Saturable Repair Models of Radiation Action in Mammalian Cells. *Radiat. Res.*, vol. 104, pp. S58–S67.

Grahn, D.; 1973: HZE Effects in Manned Spaceflight. Space Science Board, National Academy of Science, Washington, DC.

International Commission on Radiological Units and Measurements; 1986: *The Quality Factor in Radiation Protection.* Bethesda, MD: ICRU; ICRU Report 40.

Kamaratos, E.; Chang, C. K.; Wilson, J. W.; and Xu, Y. J.; 1982: Valence Bond Effects on Mean Excitation Energies for Stopping Power in Metals. *Phys. Lett.*, vol. 92A, no. 7, pp. 363–365.

Katz, R.; Ackerson, B.; Homayoonfar, M.; and Sharma, S. C.; 1971: Inactivation of Cells by Heavy Ion Bombardment. *Radiat. Res.*, vol. 47, pp. 402–425.

Katz, R.; and Cucinotta, F. A.; 1991: RBE vs. Dose for Low Doses of High-LET Radiations. *Health Physics*, vol. 60, pp. 717–718.

Köllman, K.; 1975: Dissociative Ionization of H_2, N_2, and CO by Electron Impact—Measurements of Kinetic Energy, Angular Distributions, and Appearance Potentials. *Int. J. Mass Spectrom. & Ion Phys.*, vol. 17, pp. 261–285.

Lett, J. T.; Cox, A. B.; and Story, M. D.; 1989: The Repair in the Survival of Mammalian Cells From Heavy Ion Irradiation: Approximation to the ideal case of target theory. *Adv. Space Res.* vol. 9, pp. 99–104.

Manson, S. T.; Toburen, L. H.; Madison, D. H.; and Stolterfoht, N.; 1975: Energy and Angular Distribution of Electrons Ejected From Helium by Fast Protons and Electrons: Theory and Experiment. *Phys. Review A*, vol. 12, third ser., no. 1, pp. 60–79.

Merriam, G. R.; Worgul, B. V.; Medvedovsky, C.; Zaider, M.; and Rossi, H.; 1984: Accelerated Heavy Particles on the Lens. *Radiat. Res.*, vol. 98, pp. 129–140.

Mitchison, J. M.; 1971: *The Biology of the Cell Cycle.* Cambridge University Press, Great Britian.

Ngo, F. Q. H.; Xian-Li, J.; Kalvakolanu, I.; Roberts, W.; Blue, J.; and Higgins, J.; 1990: Basic Biological Investigations of Fast Neutrons. *International Colloquium on Neutron Radiation Biology*, Rockville, MD, Nov. 5–7, 1990.

Radman, M.; Dohert, C.; Courguignon, M. F.; Doubleday, O. P.; and Letcomte, P.; 1981: High Fidelity Devices in the Reproduction of DNA in *Chromosome Damage and Repair*, E. Seeberg and K. Kleppe, eds., Plenum Press, New York.

Rustgi, M. L.; Pandy, L. N.; Wilson, J. W.; Long, S. A. T.; and Zhu, G.; 1988: Distribution of Energy in Polymers Due to Incident Electrons and Protons. *Radiat. Effects*, vol. 105, pp. 303–311.

Schaefer, Hermann J.; 1952: Exposure Hazards From Cosmic Radiation Beyond the Stratosphere and in Free Space. *J. Aviation Med.*, vol. 23, no. 4, pp. 334–344.

Schulz, George J.; 1976: A Review of Vibrational Excitation of Molecules by Electron Impact at Low Energies. *Principles of Laser Plasmas*, George Bekefi, ed., John Wiley & Sons, Inc., pp. 33–88.

Scott, B. R.; and Ainsworth, E. J.; 1980: State Vector Model for Life Shortening in Mice After Brief Exposures to Low Doses of Ionizing Radiation. *Math. Biosci.*, vol. 49, pp. 185–205.

Sinclair, W. K.; 1968: Cyclic X-ray Responses in Mammalian Cells in Vitro. *Radiat. Res.*, vol. 33, pp. 620–643.

Sinclair, W. K.; 1985: Experimental RBE Values of High LET Radiations at Low Doses and the Implications for Quality Factor Assignments. *Rad. Prot. Dos.*, vol. 13, pp. 319–326.

Tobias, C. A.; 1985: The Repair-Misrepair Model in Radiobiology: Comparison to Other Models. *Radiat. Res.*, vol. 104, pp. S77–S95.

Waligorski, M. P. R.; Sinclair, G. L.; and Katz, R.; 1987: Radiosensitivity Parameters for Neoplastic Transformations in C3H10T 1/2 CELLS. *Radiat. Res.*, vol. 111, pp. 424–437.

Wight, G. R., Van der Wiel, M. J.; and Brion, C. E.; 1976: Dipole Excitation, Ionization and Fragmentation of N_2 and CO in the 10–60 eV Region. *J. Phys. B: At. Mol. Phys.*, vol. 9, no. 4, pp. 675–689.

Wilson, J. W.; 1977a: *Analysis of the Theory of High-Energy Ion Transport.* NASA TN D-8381.

Wilson, J. W.; 1980: Nuclear-Induced Xe-Br* Photolytic Laser Model. *Appl. Phys. Lett.*, vol. 37, no. 8, pp. 695–697;.

Wilson, J. W.; and Cucinotta, F. A.; 1991: *Cellular repair/misrepair track model.* Washington, DC; NASA, Report TP-3124.

Wilson, J. W.; Cucinotta, F. A.; and Shinn, J. L.; 1991: *Multiple Lesion Track Structure Model.* Washington, DC.; NASA, Report TP- .

Wilson, J. W.; DeYoung, R. J.; and Harries, W. L.; 1979: Nuclear-Pumped ^{3}He-Ar Laser Modeling. *J. Appl. Phys.*, vol. 50, no. 3, pt. I, pp. 1226–1235.

Wilson J. W.; and Lee, J. H.; 1980: Modeling of a Solar-Pumped Iodine Laser. *Virginia J. Sci.*, vol. 31, pp. 34–38.

Wilson, J. W.; Lee, Y.; Weaver, W. R.; Humes, D. H.; and Lee, Ja H.; 1984: *Threshold Kinetics of a Solar-Simulator-Pumped Iodine Laser.* NASA TP-2241.

Wilson, J. W.; and Kamaratos, E.; 1981: Mean Excitation Energy for Molecules of Hydrogen and Carbon. *Phys. Lett.*, vol. 85A, no. 1, pp. 27–29.

Xu, Y. J.; Khandelwal, G. S.; and Wilson, J. W.; 1984b: Low-Energy Proton Stopping Power of N_2, O_2, and Water Vapor, and Deviations From Bragg's Rule. *Phys. Review A*, vol. 29, third ser., no. 6, pp. 3419–3422.

Xu, Y. J.; Khandelwal, G. S.; and Wilson, J. W.; 1985: Proton Stopping Cross Sections of Liquid Water Vapor. *Phys. Review A*, vol. 32, third ser., no. 1, pp. 629–636.

Yang, T. C.; Craise, L. M.; Mei, M.; and Tobias, C. A.; 1989: Neoplastic Cell Transformation by High LET Radiation: Molecular Mechanisms. *Adv. Space Res.*, vol. 9, pp. 131–140.